

TECHNOLOGY OF HELICAL COOLING CHANNELS
(as discussed in the Hydrogen Cryostat STTR proposal appendices)
RoI, 4/1/2005

The first five appendices discuss the unpublished results of studies of the HCC. (The basic theory of the HCC is available as an article in PRSTAB).

Appendix I is a preprint of a PAC05 paper with simulation results that show over 3 orders of magnitude 6D cooling in a HCC design based on the PRSTAB paper with two different programs.

Appendix II is a description of the new concept of a HCC with z-dependent fields.

Appendix III contains other PAC05 papers and abstracts, where the first one is a summary of our status.

Appendix IV contains the simulation of a z-dependent HCC used as a precooler.

Appendix V is a description of the same precooler in the previous appendix but used as a 6D cooling demonstration experiment, MANX. The cryostat for MANX is one of the goals of this proposal.

Appendix VI contains the first ANSYS studies of various HCC components that are relevant to the cryostat design.

Appendices VII and VIII have to do with resistivity of materials for RF to be used in HCC designs as a function of temperature, an essential parameter of cryostat designs. Appendix VII contains the known resistivity data for Al, Cu, and Be, and Appendix VIII contains a schematic of a device we would like to build to develop our capability to design high Q cavities at low temperature and high B.

Appendix IX contains the measurements of the critical currents for HTS samples and comparisons with Nb₃Sn that were done in the Fermilab Technical Division. These measurements done under this STTR grant are the first such done at Fermilab and show the temperature dependence of Bi₂Sr₂CaCu₂O₈ (BSCCO-2212) for fields up to 15 T.

Appendix X shows a device that we have built under this grant to study RF breakdown of metals and gases. It is a table-top experiment that assumes that the DC breakdown is simply related to RF breakdown.

Appendix XI contains the first two iterations of cryostat schematics for the MANX experiment, where the liquid energy absorber/refrigerant can be either hydrogen or helium. It shows that the basic goal of simplicity can be met by the proper choice of materials.

Appendix I – HCC Simulation Studies PAC05 draft preprint
Simulations of a Gas-Filled Helical
Muon Beam Cooling Channel*

Katsuya Yonehara, Daniel Kaplan (Illinois Institute of Technology, Chicago, Illinois),
Kevin Beard, S. Alex Bogacz, Yaroslav Derbenev (Jefferson Lab, Newport News, Virginia),
Rolland Johnson, Kevin Paul, Thomas Roberts (Muons, Inc, Batavia)

Abstract

A helical cooling channel (HCC) has been proposed to quickly reduce the six dimensional phase space of muon beams for muon colliders, neutrino factories, and intense muon sources. The HCC is composed of a series of RF cavities filled with dense hydrogen gas that acts as the energy absorber for ionization cooling and suppresses RF breakdown in the cavities. Magnetic solenoidal, helical dipole, and helical quadrupole coils outside of the RF cavities provide the focusing and dispersion needed for emittance exchange for the beam as it follows a helical equilibrium orbit down the HCC. In the work presented here, two Monte Carlo programs have been developed to simulate a HCC to compare with the analytic predictions and to begin the process of optimizing practical designs that could be built in the near future. We discuss the programs, the comparisons with the analytical theory, and the prospects for a HCC design with the capability to reduce the six-dimensional phase space emittance of a muon beam by a factor of over five orders of magnitude in a linear channel less than 100 meters long.

INTRODUCTION

Helical magnets have been used for some time in the control of spin precession in polarized beam devices. One advantage of helical magnets is that, in conjunction with a solenoid field, the fields are continually focusing and dispersive. Continually focusing, dispersive fields are necessary for the simultaneous transverse and longitudinal ionization cooling of muon beams.

High-pressure, hydrogen gas-filled RF cavities have been proposed to provide large gradient acceleration of muon beams. The high-pressure gas serves to suppress RF breakdown and, presumably, allows for higher RF gradients, but it also serves as the muon ionization cooling material. It is also believed that for the suppression of RF breakdown by the gas will also allow for the operation of the cavities inside strong magnetic fields.

These two concepts have been combined into a Helical Cooling Channel (HCC), consisting of helical dipole, helical quadrupole, and solenoid magnets encasing a continuous series of high-pressure, hydrogen gas-filled RF cavities. The peak RF gradient and RF phase are chosen to compensate for energy loss in the gas, maintaining the design reference energy throughout the channel.

This article shows the cooling results of simulations for such an HCC in two different simulation software packages designed for accurate modeling of muon ionization: ICOOL and G4Beamline.

SIMULATION SOFTWARE

Only a handful of simulation codes exist that can properly handle beam interactions with matter and particle decay, both of which are necessary for proper simulation of muon cooling and muon beams in general. Two such codes are ICOOL and G4Beamline.

ICOOL

ICOOL is a Monte Carlo beam tracking package, written in Fortran 77, borrowing routines to handle particle interactions with matter and decay from GEANT3. It is developed and maintained by R. Fernow [2] at Brookhaven National Laboratory specifically for development of muon colliders and neutrino factories.

G4Beamline

G4Beamline is a Monte Carlo beamline simulation package built on top of the GEANT4 toolkit [3] in C++. It is designed to have all of the particle interaction, tracking, and 3D geometry capabilities of the GEANT4 toolkit and the fully 3D graphics capability of the OpenInventor libraries, all within the framework of a beamline design program. It is developed and maintained by T. Roberts of Muons, Inc. [4].

SIMULATION RESULTS

Y. Derbenev and R. Johnson have computed the general fields and particle dynamics for helical dipole and quadrupole magnets [1]. It has already been shown that these fields match well with the measured fields from real helical magnets, such as the AGS snake [5]. Routines for computing the analytically determined fields have been written into both ICOOL and G4Beamline for simulation. The complexity of the helical channel means that a large number of parameters must be chosen by hand, and it is challenging to determine the optimal location in parameter space without more thorough simulation. For simplicity, we have started this simulation effort with a reference muon beam momentum of 200 MeV/c, a reference orbit helical pitch angle of 45 degrees (helical pitch, $\kappa = \tan 45^\circ = 1$), and a helical period of 1 meter ($\lambda = 1$ m). We have then demanded that the three cooling decrements (two transverse and one longitudinal) be equal. Under these specifications, the fields for the solenoid, helical dipole, and helical quadrupole are uniquely determined [1], listed in Table 1.

Table 1: HCC design parameters. Helical Pitch, κ , is defined as tangent of the helical pitch angle of the reference orbit. Helical field strengths are quoted at the radius of the helical reference orbit, a .

Ref. Orbit Momentum:	\mathbf{p}	200 MeV/c
Helical Ref. Orbit Pitch:	κ	1
Helical Period:	λ	1 m
Helical Ref. Orbit Radius:	\mathbf{a}	0.159 m
Solenoid Field Strength:	\mathbf{B}	5.67 T
Helical Dipole Strength:	\mathbf{b}	1.36 T
Helical Quadrupole Strength:	\mathbf{b}'	-1.02 T/m
Helical Single-Period Transverse Tunes:	\mathbf{Q}_+ \mathbf{Q}_-	0.905 0.774
Transition Momentum	\mathbf{p}_t	49.2 MeV/c
RF Frequency:	\mathbf{f}_{RF}	200 MHz
RF Phase:	ϕ_{RF}	140°
RF Gradient:	\mathbf{E}_{RF}	33 MV/m

High-pressure, gaseous hydrogen-filled RF cavities [6] are placed inside the helical magnets. We assume 100 atm gaseous hydrogen at 77 K inside the cavities, which corresponds to half the density of liquid hydrogen. After considering the fact that the particle trajectories are not aligned with the central axis of the cavities (i.e., they are helical), an average RF gradient of 21 MV/m must be applied to the beam to compensate for energy loss in the gas. Since we are above transition, we select an RF phase of 140° such that the peak RF gradient of our cavities must be 33 MV/m. The simulations assume sinusoidal time-dependence but no radial dependence in the RF fields. Experiments at Fermilab's Mucool Test Area (MTA) have been proposed to test the operation of cavities under similar conditions [7].

*Work supported in part by DOE STTR/SBIR grants DE-FG02-02ER86145 and 03ER83722.

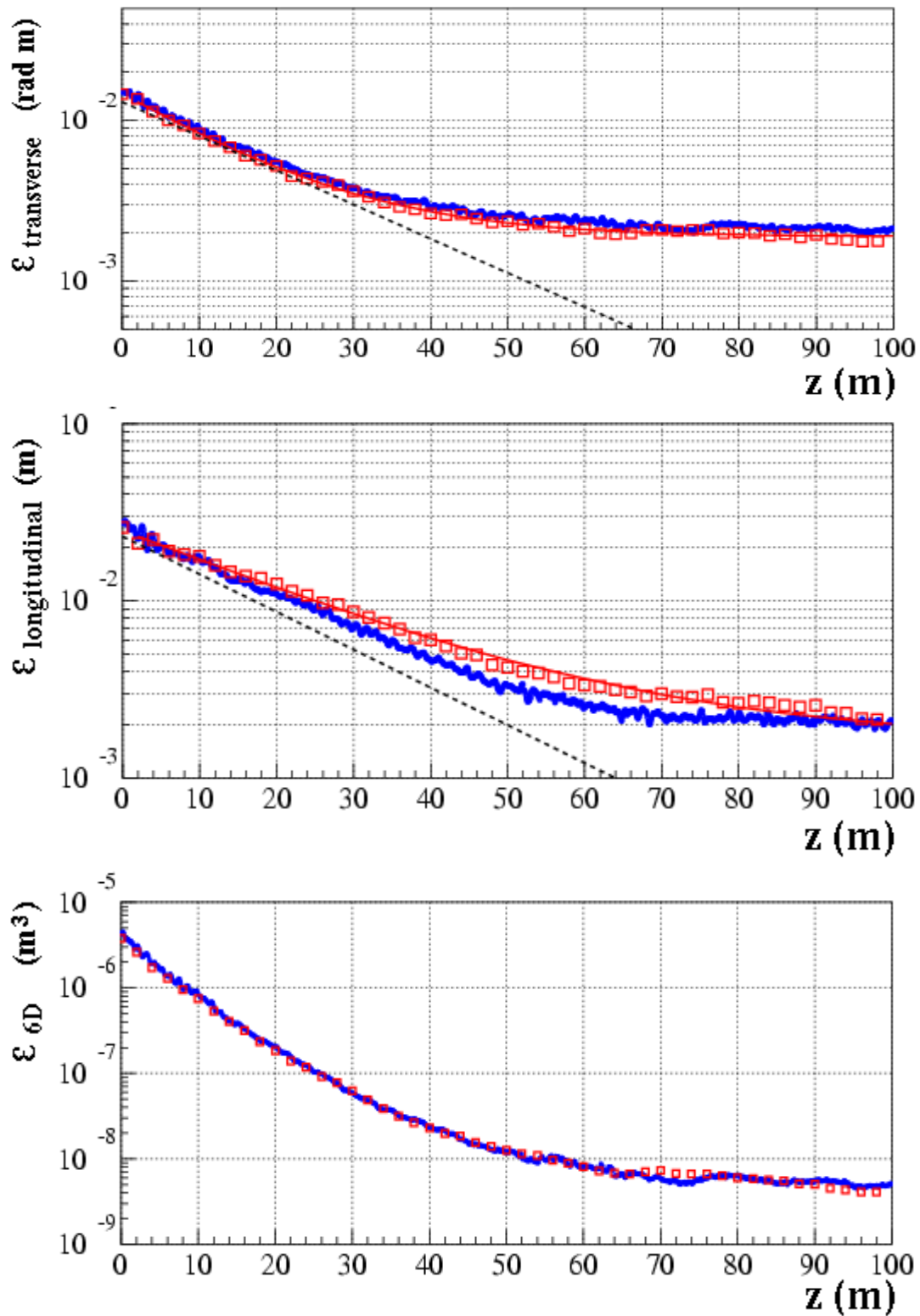


Figure 1: These plots show the evolution of normalized emittance, as calculated from the ICOOL post-processing tool ECALC9, down the length of the channel. Red dots represent simulation results from G4Beamline, and blue dots represent the simulation results from ICOOL. An exponential curve (red) with a constant offset is fitted to the G4Beamline data in both the longitudinal and transverse plots above, from which fitted values for the cooling decrements have been found. The black dotted lines in the transverse and longitudinal plots represent the theoretically predicted exponential cooling, neglecting the equilibrium emittance.

Figure 1 shows the evolution of the normalized transverse, longitudinal, and six-dimensional emittance down the length of the HCC, as calculated by the ICOOL post-processing tool ECALC9 [8]. Perfect matching into the channel is assumed. Results are found by considering only the surviving subset of muons from a large beam that saturates the acceptance of the channel, where survival is determined by whether the muon reaches the end of the channel. We see fairly good agreement between the two simulation codes. We have fitted the transverse and longitudinal emittances with offset exponential decay curves, and from these fits we extract approximate cooling decrements of $\Lambda_{\text{trans}} = 0.069 \text{ m}^{-1}$ and $\Lambda_{\text{long}} = 0.041 \text{ m}^{-1}$. There is a slight discrepancy between these cooling decrements and the theoretically predicted cooling decrements, $\Lambda_{\text{trans}} = \Lambda_{\text{long}} = 0.049 \text{ m}^{-1}$. The initial six-dimensional acceptance of the channel is very large, around 4 cm^3 (15 mm transverse, 27 mm longitudinal), comparable to the initial emittance of the muon beam considered in the Neutrino Factory Feasibility Study 2a. The HCC cools the beam by a factor of approximately 800 over a channel length of 100 m, down to a six-dimensional emittance of 5 mm^3 (2 mm transverse, 2 mm longitudinal).

Preliminary simulations suggest even greater cooling with slightly different design parameters. By changing the reference orbit momentum to 250 MeV/c, and changing the field strengths accordingly, cooling factors of close to 5000 have been observed. The cooling decrements for this design, however, have not yet been measured.

FUTURE PROSPECTS

With different design parameter choices, it is, in principle, possible to create a helical cooling channel that has a lower equilibrium emittance and smaller acceptance. Such a helical cooling channel can be used following the channel described in the previous section. To be more efficient, one might consider an HCC equivalent to that described in the previous section but with a shorter length, followed by a series of HCC's with sequentially smaller equilibrium emittances and acceptances. Then, we more efficiently take advantage of the faster cooling rate achieved by a beam that is further from equilibrium. Such a design can maximize cooling and minimize the required length of the channel.

Finalized designs depend on the feasibility of the high-pressure, hydrogen gas-filled RF cavities [6] to be determined in future experiments [7]. If the required gradients are not achievable in such high fields, then it may be possible to create a channel that alternates between the gas-filled helical magnets and high-gradient, gas-filled RF. Such a design would not be as efficient, but it could still achieve dramatic cooling. Other complications that may be uncovered during the proposed experiments could require alternative designs, but the design discussed in the prior section would be the most efficient.

References

- [1] Y. Derbenev and R. Johnson, "Six-dimensional muon beam cooling using a homogeneous absorber," PRSTAB, something-something.
- [2] R. Fernow, ICOOL...
- [3] GEANT4 Toolkit...
- [4] T. Roberts, G4Beamline...
- [5] Citation for comparison between analytical fields and measured fields for the AGS snake.
- [6] Hydrogen gas-filled RF cavities.
- [7] Proposed MTA HPGH2 experiments.
- [8] ECALC9.

Appendix II – Momentum Dependent HCC

New Idea Based on a Helical Cooling Channel with Continuous Absorber

As discussed in the overview section above and the previous Appendix, the results of analytical and numerical simulation calculations of 6D cooling based on a HCC have been very encouraging. In these studies, a long HCC encompasses a series of contiguous RF cavities that are filled with dense hydrogen gas so that the beam energy is kept almost constant, where the RF continuously compensates for the energy loss in the absorber. In this case, the strengths of the magnetic solenoid and helical dipole and quadrupole magnets of the HCC are also held constant. This feature of the HCC channel is exploited in the mathematical derivation of its properties, where the transverse field is subject only to a simple rotation about the solenoid axis as a function of distance, z , along the channel. This rotational invariance leads to a z and time-independent Hamiltonian, which in turn allows the dynamical and cooling behavior of the channel to be examined in great detail. An important relationship between the momentum, p , for an equilibrium orbit at a given radius, a , and magnetic field parameters is derived in reference [3] (also appended to this proposal);

$$p(a) = \frac{\sqrt{1 + \kappa^2}}{k} \left[B - \frac{1 + \kappa^2}{\kappa} b \right], \quad (\text{III.12})$$

where B is the solenoid strength, b is the helical dipole strength at the particle position, k is the helix wave number ($k = 2\pi / \lambda$), and $\kappa \equiv ka = p_{\perp} / p_z$ is the tangent of the helix pitch angle.

The new idea that is the basis for many of the ideas in this proposal is that equation (III.12) is not just a description of the requirements for a simple HCC. It is also a recipe to manipulate field parameters to maintain stability for cases where you would like the momentum and/or radius of the equilibrium orbit to change for various purposes. Examples of these purposes that we have examined so far include:

- 1) precooling devices to cool a muon beam as it decelerates by energy loss in a continuous, homogeneous absorber, where the cooling can be all transverse, all longitudinal, or any combination (the first study of this use is described in Appendix I, below),
- 2) a device similar to a precooler, but used as a muon cooling demonstration experiment (this MANX project is discussed in much more detail below),
- 3) a transition section between two HCC sections with different dimensions as when the RF frequency can be increased once the beam has been cooled sufficiently to allow smaller and more effective cavities and magnetic coils, and
- 4) as an alternative to the original HCC filled with pressurized RF cavities. In this alternate case, muons would lose a few hundred MeV/c in a HCC section with momentum dependent fields and then pass through several RF cavities to replenish the lost energy, where this sequence could be repeated several times.

Additional constraints to the equation above are needed to determine the cooling properties of the channel. For example, to achieve equal cooling decrements in the two transverse and the longitudinal coordinates, the condition is:

$$q \equiv \frac{k_c}{k} - 1 = \beta \sqrt{\frac{1 + \kappa^2}{3 - \beta^2}}, \quad (\text{IV.21})$$

where $k_c = B\sqrt{1 + \kappa^2}/p$ is related to the cyclotron motion, q is an effective field index, and $\beta = v/c$.

Another example, to achieve a condition where all the cooling is in the longitudinal direction, is to require that: $\hat{D} \equiv \frac{p}{a} \frac{da}{dp} = 2 \frac{1 + \kappa^2}{\kappa^2}$ and $q = 0$.

We have developed EXCEL spreadsheets to use for the modeling of the channels that we simulate. An example showing one of the calculations for a MANX experiment with equal cooling decrements and an initial momentum of 400 MeV/c is shown below. The references to the paper on the theory of the HCC by line number in the Mucool Note 284 are off by one due to a revision of the paper done after the spreadsheet was created. This particular example was to investigate the case where the helical dipole field strength (b) was held constant while the solenoidal field strength (B) was varied in order to keep the equilibrium orbit (a) constant as the momentum was reduced by a liquid hydrogen absorber.

Helical Cooling Channel Simulation Parameters and Fields

parameter	unit	reference	Initial	1 m	2 m	3 m	4 m	5 m	6 m
p	MeV/c		400	369.8335	339.4965	308.8762	277.8007	245.9953	212.9867
KE	MeV	Kinematic	308.0598	278.9708	249.8986	220.7884	191.5559	162.0669	132.0949
β		Kinematic	0.966838	0.961529	0.954826	0.946172	0.934677	0.918829	0.895825
γ		Kinematic	3.915576	3.640268	3.36512	3.089612	2.812946	2.533853	2.250188
T_{\max}	MeV	PDG 27.2	14.11219	12.09491	10.2183	8.480067	6.877445	5.407005	4.064179
dE/dx	MeV/m	PDG 27.1	29.089	29.07217	29.11024	29.23248	29.48894	29.97207	30.87247
λ	m		1	1	1	1	1	1	1
k	1/m	$2\pi/\lambda$	6.28318	6.28318	6.28318	6.28318	6.28318	6.28318	6.28318
a	m		0.159155	0.159155	0.159155	0.159155	0.159155	0.159155	0.159155
κ		ka	1	1	1	1	1	1	1
p_T	MeV/c	from $\kappa = p_T / p_z$	282.8427	261.5117	240.0603	218.4084	196.4348	173.9449	150.6044
p_z	MeV/c		282.8427	261.5117	240.0603	218.4084	196.4348	173.9449	150.6044
b	T		2.818113	2.818113	2.818113	2.818113	2.818113	2.818113	2.818113
B	T	MUC-284 III.9	11.56006	11.11331	10.66403	10.21056	9.750343	9.279317	8.790474
k_c	1/m	zeB/ p_z	12.2613	12.74892	13.32669	14.02495	14.89096	16.00389	17.5104
q		$(k_c/k) - 1$	0.951448	1.029056	1.121011	1.232142	1.369972	1.5471	1.786869
$(\partial b/\partial a)$	T/m		-3.041915	-3.04192	-3.04192	-3.04192	-3.04192	-3.04192	-3.04192
g		MUC-284 III.11	0.163454	0.176786	0.192583	0.211675	0.235354	0.265783	0.306974

A		$b = A b_d + B b_q$	1.130318	1.130318	1.130318	1.130318	1.130318	1.130318	1.130318
B			0.10965	0.10965	0.10965	0.10965	0.10965	0.10965	0.10965
C		$(\partial b/\partial a) = C b_d + D b_q$	1.705854	1.705854	1.705854	1.705854	1.705854	1.705854	1.705854
D			1.114428	1.114428	1.114428	1.114428	1.114428	1.114428	1.114428
b_d	T	MUC-284 III.2-3	3.238943	3.238943	3.238943	3.238943	3.238943	3.238943	3.238943
b_q	T/m	MUC-284 III.2-3	-7.687419	-7.68742	-7.68742	-7.68742	-7.68742	-7.68742	-7.68742
b₁	T	ICOOL Parameter	3.238943	3.238943	3.238943	3.238943	3.238943	3.238943	3.238943
b₂	T	ICOOL Parameter	-0.611746	-0.61175	-0.61175	-0.61175	-0.61175	-0.61175	-0.61175
r_{bp}	m	Beampipe Radius	0.3	0.3	0.3	0.3	0.3	0.3	0.3
b_φ(r_{bp})_{max}	T	MUC-284 III.2-3	1.614288	1.614288	1.614288	1.614288	1.614288	1.614288	1.614288
b_φ(r_{bp})_{dip}	T	MUC-284 III.2-3	8.736191	8.736191	8.736191	8.736191	8.736191	8.736191	8.736191
b_φ(r_{bp})_{quad}	T	MUC-284 III.2-3	-6.399319	-6.39932	-6.39932	-6.39932	-6.39932	-6.39932	-6.39932
 b_z(r_{bp})_{max} 	T	MUC-284 III.2-3	14.60292	14.15617	13.70689	13.25342	12.7932	12.32218	11.83333
Ḑ⁻¹		MUC-284 III.10	0.663454	0.676786	0.692583	0.711675	0.735354	0.765783	0.806974
Ḑ			1.507265	1.477572	1.443869	1.405135	1.35989	1.305853	1.239197
G		MUC-284 III.17	0.522798	0.576804	0.643014	0.726241	0.834346	0.981211	1.194237
R		MUC-284 III.18	0.726313	0.764739	0.814166	0.879543	0.969206	1.09838	1.298225
R² - G		MUC-284 III.19-20	0.004733	0.008021	0.019853	0.047356	0.105014	0.225227	0.491151
R²/G		MUC-284 III.19-20	1.009054	1.013907	1.030876	1.065207	1.125864	1.22954	1.411268
Q₊		MUC-284 II.19	0.891691	0.924284	0.977276	1.047453	1.137218	1.254177	1.413876
Q₋		MUC-284 II.19	0.810872	0.821691	0.820527	0.813591	0.80321	0.789809	0.772919
k₊		kQ ₊	5.602655	5.807444	6.140401	6.581334	7.145346	7.880221	8.88364
k₋		kQ ₋	5.094858	5.162835	5.155518	5.111936	5.046715	4.962515	4.856386
α₊		MUC-284 pg 23	-5.423453	12.21888	4.338202	3.32109	3.015964	2.950748	3.029915
α₋		MUC-284 pg 23	0.244661	-0.11078	-0.3193	-0.42858	-0.48764	-0.51904	-0.53267
η		MUC-284 III.48	0.275109	0.289881	0.305897	0.323045	0.34083	0.357715	0.369014
γ_t		MUC-284 pg 29	0.753632	0.738786	0.721935	0.702568	0.679945	0.652926	0.619599
log		PDG 27.1	12.60721	12.46191	12.30486	12.13356	11.94441	11.73192	11.48684
Λ₀	1/m	MUC-284 pg 31	0.075217	0.081754	0.089802	0.100026	0.11357	0.132604	0.161806
(dF/dE)	1/m	MUC-284 IV.3	0.001393	-0.00013	-0.00244	-0.00602	-0.01179	-0.02167	-0.04021
Λ_v	1/m	MUC-284 IV.7	0.058079	0.060265	0.062392	0.064259	0.065432	0.064907	0.06005
Λ₊	1/m	MUC-284 IV.15	0.046874	0.094665	0.126253	0.151538	0.179646	0.216994	0.273391
Λ₋	1/m	MUC-284 IV.15	0.046874	0.008444	-0.01148	-0.02176	-0.02973	-0.03837	-0.05003
Λ₊ + Λ₋	1/m	Λ ₊ + Λ ₋	0.093748	0.103109	0.114773	0.129776	0.149919	0.178627	0.223358
Λ₊ + Λ₋	1/m	MUC-284 IV.16	0.093748	0.103109	0.114773	0.129776	0.149919	0.178627	0.223358
Λ	1/m	Λ ₊ + Λ ₋ + Λ _v	0.151827	0.163374	0.177165	0.194035	0.215351	0.243533	0.283407
Λ	1/m	MUC-284 IV.17	0.140622	0.151169	0.163744	0.179094	0.198434	0.2239	0.2597

Γ_+		<i>MUC-284 V.10</i>	3.762258	2.407447	2.675681	3.189537	3.681118	4.159399	4.665062
Γ_-		<i>MUC-284 V.10</i>	10.79056	11.54389	10.71734	9.687535	8.721413	7.808748	6.907089
ϵ_+	<i>mm rad</i>	<i>MUC-284 V.9</i>	0.48083	0.159029	0.136875	0.140177	0.141221	0.137798	0.129881
ϵ_-	<i>mm rad</i>	<i>MUC-284 V.9</i>	1.516526	9.616448	-7.1811	-3.81707	-2.86281	-2.32339	-1.92214

Appendix III – Muons, Inc. PAC05 Submissions.

Recent Innovations in Muon Beam Cooling and Prospects for Muon Colliders*

Rolland P. Johnson[#], Mohammad Alsharo'a, Pierrick M. Hanlet, Robert Hartline, Moyses Kuchnir, Kevin Paul, Thomas Roberts (Muons, Inc, Batavia), Charles Ankenbrandt, Emanuela Barzi, Licia del Frate, Ivan Gonin, Alfred Moretti, David Neuffer, Milorad Popovic, Gennady Romanov, Daniele Turrioni, Victor Yarba (Fermilab, Batavia, Illinois), Daniel Kaplan, Katsuya Yonehara (Illinois Institute of Technology, Chicago, Illinois), Kevin Beard, S. Alex Bogacz, Yaroslav Derbenev (Jefferson Lab, Newport News, Virginia)

Abstract

New ideas are being developed to cool muon beams for colliders, neutrino factories, and muon experiments. Analytical and simulation studies have confirmed that a six-dimensional (6D) cooling channel based on helical magnets surrounding RF cavities filled with dense hydrogen gas can be used to achieve very small emittances. This helical cooling channel (HCC) has solenoidal, helical dipole, and helical quadrupole magnetic fields to generate emittance exchange and achieve 6D emittance reduction of over 3 orders of magnitude in a 100 m segment. Three such sequential HCC segments, where the RF frequencies are increased and transverse dimensions reduced as the beams become cooler, implies a 6D emittance reduction of almost six orders of magnitude. Two new post-cooling ideas then can be employed to reduce transverse emittances to one or two mm-mr, which allows high luminosity with fewer muons than previously imagined. We describe the new post-cooling ideas as well as a new precooling idea based on a HCC with z -dependent fields that can be used as an exceptional 6D cooling demonstration experiment.

INTRODUCTION

The projects discussed below are to improve the cooling of intense muon beams, which could reduce costs of neutrino factories and facilitate designs of high-luminosity muon colliders. Taken together, these SBIR and STTR projects represent a coherent, innovative program to develop a muon source to be used in these and other projects.

HIGH-PRESSURE RF CAVITIES

A gaseous energy absorber enables an entirely new technology to generate high accelerating gradients for muons by using the high-pressure region of the Paschen curve [1]. This idea of filling RF cavities with gas is new for particle accelerators and is only possible for muons because they do not scatter as do strongly interacting protons or shower as

do less-massive electrons. Measurements by Muons, Inc. and IIT at Fermilab have demonstrated that hydrogen gas suppresses RF breakdown very well, about a factor six better than helium at the same temperature and pressure. Consequently, much more gradient is possible in a hydrogen-filled RF cavity than is needed to overcome the ionization energy loss, provided one can supply the required RF power. Hydrogen is also twice as good as helium in ionization cooling effectiveness, viscosity, and heat capacity. Present research efforts include tests of pressurized RF Cavities in magnetic fields and high radiation environments and the use of new cavity construction materials [2], including beryllium RF windows for improved cavity performance [3].

Combined Capture, Phase Rotation, Cooling

High-pressure RF cavities near the pion production target can be used to simultaneously capture, bunch rotate, and cool the muon beam as it emerges from the decaying pions [4]. This project is an R & D effort to develop RF cavities that will operate in the extreme conditions near a production target and an effort to simulate the simultaneous capture, phase rotation, and cooling of muons as they are created from pion decay.

HELICAL COOLING CHANNELS

The idea of pressurized RF cavities led to the concept of a cooling channel filled with a continuous homogeneous absorber to provide longitudinal ionization cooling by exploiting the path length (and therefore energy loss) correlation with momentum in a magnetic channel with positive dispersion. Using this approach in a helical cooling channel creates emittance exchange and excellent 6D muon beam cooling [5]. Figure 1 shows a comparison of results of G4BL and ICOOL simulations of a HCC filled with 200 MHz RF cavities pressurized with hydrogen gas to a density corresponding to half the density of liquid hydrogen. The simulations agree with each other and show nearly equal values of the three cooling decrements and a factor of 5000 reduction of 6D emittance [6]. For a complete cooling channel, there would be three or four 20 m long segments, each with higher RF frequency, smaller dimensions,

* Supported in part by DOE SBIR/STTR grants DE-FG02-02ER86145, 03ER83722, 04ER84015, 04ER86191, and 04ER84016

[#] rol@muonsinc.com

and higher magnetic fields as the beam becomes cooler.

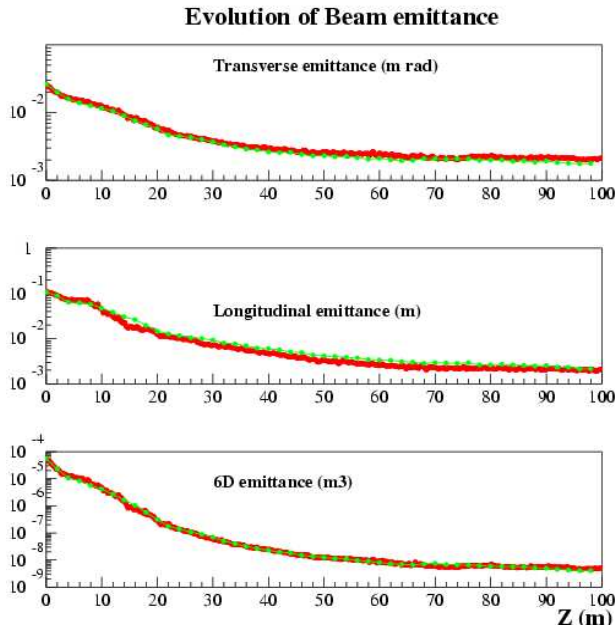


Fig. 1. G4BL (Red) and ICOOL (Green) simulation comparisons of a HCC segment filled with 200 MHz RF cavities pressurized with dense gaseous hydrogen.

MOMENTUM DEPENDENT HCC

The HCC concept has now been extended to have momentum-dependent magnetic field strengths for several new applications. Two examples are a 6D pre-cooler which will also serve as a 6D Muon Collider And Neutrino Factory muon beam cooling demonstration experiment, MANX [7], which is being designed to follow MICE [8].

Pre-cooler and Sequential RF

The conceptual change that allowed it to become a z or momentum-dependent device has made the HCC a potential work-horse for different components of the muon beam cooling channel. For example, by filling the HCC with liquid hydrogen or liquid helium, the beam can be decelerated and cooled by ionization energy loss over more than 100 MeV/c, then reaccelerated by a series of RF cavities (pressurized or conventional). The HCC magnet parameters must be varied to match the momentum of the beam as it slows down. Filled with liquid, the HCC with momentum dependent field parameters followed by RF cavities can be a 6D pre-cooler, a 6D demonstration experiment, or an alternative to the original gas-filled HCC (where the momentum is kept almost constant). Figure 2 shows a G4BL display of a HCC simulation of a 6 m pre-cooler that follows a 40 m HCC decay channel. Filled with gas,

the HCC with variable magnetic field parameters can be used as a transition between original HCC sections with different RF frequencies and fields.

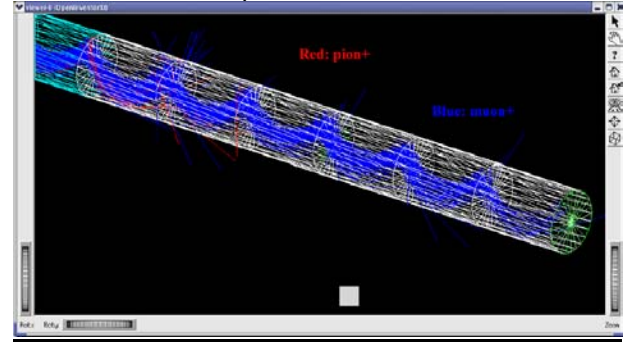


Fig. 2. G4BL Openinventor display of a liquid hydrogen filled HCC without RF used as a pre-cooler.

MANX

Simulation results in figure 3 show that part of the pre-cooler in figure 2 can serve as the MANX 6D cooling demonstration. The normalized longitudinal emittance is reduced by a factor of 1.7 as are each of the transverse emittances in a HCC segment of 5 m length. This total 6D emittance reduction of a factor of 5.5 can be compared to the expected MICE cooling effect of about 10% with no longitudinal cooling. Present studies are to develop a simulation of a MANX design that incorporates the MICE spectrometers and the RAL beamline.

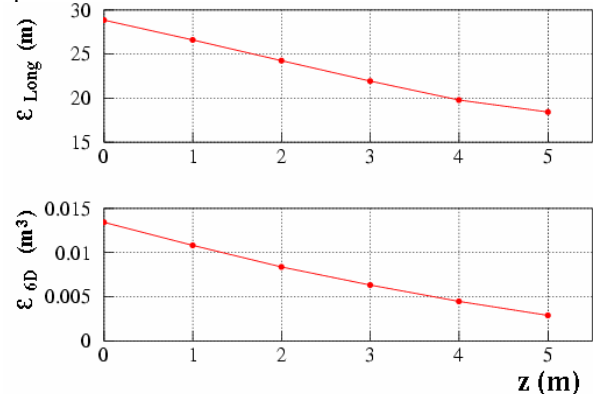


Fig. 3. Simulated MANX cooling of (TOP) normalized longitudinal and (BOTTOM) 6D emittances in a 5 m long HCC filled with liquid hydrogen.

HTS and H₂ Cryostats

Two very interesting technological aspects of HCC designs involve the potential use of HTS to achieve very high fields and the use of hydrogen to act simultaneously as refrigerant, ionization energy absorber, and RF breakdown suppressant [9].

POST COOLING TECHNIQUES

The excellent cooling that we expect to achieve using the HCC in its various incarnations will bring normalized transverse emittances down to values of a few hundred mm-mr, which is considerably larger than is usual for electron or proton colliders. For collider applications, it has been assumed that a large intensity will make up for this rather large beam size and the emphasis on muon beam technology has been on 4 MW proton drivers and clever production targets.

The two innovations below, which are now under development, together have the potential to reduce each muon beam normalized transverse emittance another two orders of magnitude to just a few mm-mr, not unlike those presently used in colliders.

Parametric-resonance Ionization Cooling

Parametric-resonance Ionization Cooling (PIC) [10], requires a half integer resonance to be induced in a ring or beam line such that the normal elliptical motion of particles in $x - x'$ phase space becomes hyperbolic, with particles moving to smaller x and larger x' as they pass down the beam line. (This is almost identical to the technique used for half integer extraction from a synchrotron where the hyperbolic trajectories go to small x' and larger x to pass the wires of an extraction septum.) Thin absorbers placed at the focal points of the channel then cool the angular divergence of the beam by the usual ionization cooling mechanism where each absorber is followed by RF cavities. Thus in PIC the phase space area is reduced in x due to the dynamics of the parametric resonance and x' is reduced or constrained by ionization cooling.

The basic theory of PIC is being developed to include aberrations and higher order effects. Simulations using linear channels of quadrupoles, solenoids, or HCC's are now underway [11].

Reverse Emittance Exchange

A muon beam that is well cooled at one or two hundred MeV/c will have its unnormalized emittance reduced by a factor of a thousand or more at 100 or more GeV/c collider energy. At the interaction point in the collider the bunch length would then be much shorter than the IR focal length. In reverse emittance exchange, we propose to repartition the emittances to lengthen the bunch length at collider energy and narrow the transverse emittances using beryllium wedge energy absorbers.

Preliminary calculations show that two stages of reverse emittance exchange, one at low energy and one at a higher energy before energy straggling

becomes significant, can improve each transverse emittance by an order of magnitude.

CONCLUSIONS

The path to an affordable neutrino factory and a compelling design of a muon collider has complementary projects that we are pursuing with SBIR and STTR grants and proposals, many of which are described in these proceedings.

We are exploring the possible variations of HCC designs, where the original one has shown the promise of several orders of magnitude of 6D cooling and the new HCC ideas with momentum dependent magnetic fields are encouraging. The plan for a 6D cooling experiment using a HCC is taking shape, with a cooling effect that we believe will be striking.

The new post cooling ideas may allow us to have muon beams with transverse emittances as small as those that are now common in the collider world. If this can be accomplished, the number of muons needed in a collider can be reduced by an order of magnitude (for the same luminosity, which is limited by the beam-beam tune shift). The consequences of reduced muon intensity are very significant: the proton driver and targeting requirements can be met with existing machines and technology, the detector backgrounds from muon decay electrons are reduced by a factor of ten, and the site boundary radiation levels due to neutrino interactions in the soil are also reduced by the same factor.

Another important consequence of excellent 6D beam cooling is that the cost of acceleration of muons to collider or neutrino factory energy can be reduced by using higher RF frequency and smaller magnetic channel dimensions, for example by using a recirculating Linac with TESLA RF.

REFERENCES

[1] R. P. Johnson et al. LINAC2004, www.muonsinc.com/TU203.pdf

[2] Pierrick M. Hanlet et al., Studies of RF Breakdown of Metals in Dense Gases, this conference

[3] Mohammad Alsharo'a et al., Beryllium RF Windows for Gaseous Cavities for Muon Acceleration, this conference

[4] Kevin Paul et al., Simultaneous bunching and precooling muon beams with gas-filled RF cavities, this conference

[⁵] Y. Derbenev and R. P. Johnson, Submitted to PRSTAB, <http://www.mucool.fnal.gov/mcnotes/public/pdf/muc0284/muc0284.pdf>.

[⁶] Katsuya Yonehara, et al., Simulations of a Gas-Filled Helical Muon Beam Cooling Channel, this conference

[⁷] Thomas J. Roberts et al., A Muon Cooling Demonstration Experiment Using Gaseous Hydrogen, this conference

[⁸] M. A. Cummings et al., New Technology in Hydrogen Absorbers, and Michael Green, Progress on the Cryogenic System for a Liquid Absorber in the MICE Cooling Channel, this conference.

[⁹] Emanuela Barzi et al., Novel Muon Cooling Channels Using Hydrogen Refrigeration and HT Superconductor, this conference

[¹⁰] Yaroslav Derbenev et al., Ionization Cooling Using a Parametric Resonance, this conference

[¹¹] Kevin Beard et al., Simulations of Parametric Resonance Ionization Cooling of Muon Beams, this conference

ID: 1247 Simulations of a Gas-Filled Helical Muon Beam Cooling Channel

Authors Katsuya Yonehara, Daniel Kaplan (Illinois Institute of Technology, Chicago, Illinois), Kevin Beard, S. Alex Bogacz, Yaroslav Derbenev (Jefferson Lab, Newport News, Virginia), Rolland Johnson, Kevin Paul, Thomas Roberts (Muons, Inc, Batavia)

Presenter Katsuya Yonehara (Illinois Institute of Technology, Chicago, Illinois)

Abstract A helical cooling channel (HCC) has been proposed to quickly reduce the six dimensional phase space of muon beams for muon colliders, neutrino factories, and intense muon sources. The HCC is composed of a series of RF cavities filled with dense hydrogen gas that acts as the energy absorber for ionization cooling and suppresses RF breakdown in the cavities. Magnetic solenoidal, helical dipole, and helical quadrupole coils outside of the RF cavities provide the focusing and dispersion needed for the emittance exchange for the beam as it follows a helical equilibrium orbit down the HCC. In the work presented here, two Monte Carlo programs have been developed to simulate a HCC to compare with the analytic predictions and to begin the process of optimizing practical designs that could be built in the near future. We discuss the programs, the comparisons with the analytical theory, and the prospects for a HCC design with the capability to reduce the six-dimensional phase space emittance of a muon beam by a factor of over five orders of magnitude in a linear channel less than 100 meters long.

Funding Agency This work was supported in part by DOE STTR/SBIR grants DE-FG02-02ER86145 and 03ER83722.

Type of Presentation Poster

ID: 1248 Ionization Cooling Using a Parametric Resonance

Authors Yaroslav Derbenev (Jefferson Lab, Newport News, Virginia), Rolland Johnson (Muons, Inc, Batavia)

Presenter Yaroslav Derbenev (Jefferson Lab, Newport News, Virginia)

Abstract Muon collider luminosity depends on the number of muons in the storage ring and on the transverse size of the beams in collision. Ionization cooling as it is presently envisioned will not cool the beam sizes sufficiently well to provide adequate luminosity without large muon intensities. A new idea to combine ionization cooling with parametric resonances has been developed that will lead to beams with much smaller sizes so that high luminosity in a muon collider can be achieved with fewer muons. In the linear channel described here, a half integer resonance is induced such that the normal elliptical motion of particles in $x-x'$ phase space becomes hyperbolic, with particles moving to smaller x and larger x' as they pass down the channel. Thin absorbers placed at the focal points of the channel then cool the angular divergence of the beam by the usual ionization cooling mechanism where each absorber is followed by RF cavities. We discuss the theory of Parametric-resonance Ionization Cooling, including the sensitivity to aberrations and the need to start with a beam that has already been cooled adequately.

Funding Agency This work was supported in part by DOE SBIR grant DE-FG02-04ER84016.

Type of Presentation Poster

ID: 1249 Simulations of Parametric Resonance Ionization Cooling of Muon Beams

Authors Kevin Beard, S. Alex Bogacz, Yaroslav Derbenev (Jefferson Lab, Newport News, Virginia), Katsuya Yonehara (Illinois Institute of Technology, Chicago, Illinois), Rolland Johnson, Kevin Paul, Thomas Roberts (Muons, Inc, Batavia)

Presenter Kevin Beard (Jefferson Lab, Newport News, Virginia)

Abstract The technique of using a parametric resonance to allow better ionization cooling is being developed to create small beams so that high collider luminosity can be achieved with fewer muons. In the linear channel that is studied in this effort, a half integer resonance is induced such that the normal elliptical motion of particles in $x-x'$ phase space becomes hyperbolic, with particles moving to smaller x and larger x' as they pass down the channel. Thin absorbers placed at the focal points of the channel then cool the angular divergence of the beam by the usual ionization cooling mechanism where each absorber is followed by RF cavities. Thus the phase space of the beam is compressed in transverse position by the dynamics of the resonance and its angular divergence is compressed by the ionization cooling mechanism. We report the first results of simulations of this process, including comparisons to theoretical cooling rates and studies of sensitivity to variations in absorber thickness and initial beam conditions.

Funding Agency This work was supported in part by DOE SBIR grants DE-FG02-03ER83722, and 04ER84016.

Type of Presentation Poster

ID: 1250 Studies of RF Breakdown of Metals in Dense Gases

Authors Pierrick M. Hanlet, Mohammad Alsharo'a, Rolland Johnson, Moyses Kuchnir (Muons, Inc, Batavia), Charles Ankenbrandt, Alfred Moretti, Milorad Popovic (Fermilab, Batavia, Illinois), Daniel Kaplan, Katsuya Yonehara (Illinois Institute of Technology, Chicago, Illinois)

Presenter Pierrick M. Hanlet (Muons, Inc, Batavia)

Abstract A study of RF breakdown of metals in gases has begun as part of a program to develop RF cavities filled with dense hydrogen gas to be used for muon ionization cooling. A pressurized 800 MHz test cell has been used at Fermilab to compare the conditioning and breakdown behavior of copper, molybdenum, chromium, and beryllium electrodes as functions of hydrogen and helium gas density. These results are compared to the predicted or known RF breakdown behavior of these metals in vacuum.

Funding Agency This work was supported in part by DOE STTR grant DE-FG02-02ER86145.

Type of Presentation Poster

ID: 1251 Novel Muon Cooling Channels Using Hydrogen Refrigeration and High Temperature Superconductor

Authors Emanuela Barzi, Daniele Turrioni (Fermilab, Batavia, Illinois), Rolland Johnson, Moyses Kuchnir (Muons, Inc, Batavia)

Presenter Emanuela Barzi (Fermilab, Batavia, Illinois)

Abstract Ionization cooling, a method for shrinking the size of a muon beam, requires a low Z energy absorber, high-field magnets, and high gradient RF. It is proposed to use one gaseous hydrogen system to provide ionization energy loss for muon beam cooling, breakdown suppression for pressurized high-gradient RF cavities, and refrigeration for superconducting magnets and cold RF cavities. We report progress on the design of a cryostat and refrigeration system that circulates hydrogen through magnetic coils, RF cavities, and the absorber volume to achieve a safe, robust means to enable exceptionally bright muon beams. We find that the design can be greatly simplified if a high temperature superconductor can be used that has the capability to carry adequate current in fields above 10 T at a temperature above 33 K, the critical temperature of hydrogen.

Funding Agency This work was supported in part by DOE STTR grant DE-FG02-04ER86191.

ID: 1252 A Muon Cooling Demonstration Experiment Using Gaseous Hydrogen

Authors Thomas Roberts, Mohammad Alsharo'a, Pierrick M. Hanlet, Rolland Johnson, Moyses Kuchnir, Kevin Paul (Muons, Inc, Batavia), Charles Ankenbrandt, Alfred Moretti, Milorad Popovic, Victor Yarba (Fermilab, Batavia, Illinois), Daniel Kaplan, Katsuya Yonehara (Illinois Institute of Technology, Chicago, Illinois)

Presenter Thomas Roberts (Muons, Inc, Batavia)

Abstract Most ionization cooling schemes now under consideration are based on using many large flasks of liquid hydrogen energy-absorber. One important example is the proposed Muon Ionization Cooling Experiment (MICE). In the work reported here, potential muon cooling demonstration experiments based on a gaseous energy absorber are discussed. For transverse cooling, the gaseous absorber leads to a conceptually simpler design than with liquid flasks and has better cooling and several engineering advantages, including the potential of higher accelerating gradients. We report on the development of the concept of an ionization-cooling channel based on a gaseous absorber with high-gradient RF cavities and the design of a channel section suitable for testing in a muon beam. We also discuss the possibility of a six-dimensional cooling demonstration experiment based on a cooling channel using solenoidal and helical dipole magnetic fields.

Funding Agency This work was supported in part by DOE SBIR grant DE-FG02-04ER84015.

Type of Presentation Poster

ID: 1253 Beryllium RF Windows for Gaseous Cavities for Muon Acceleration

Authors Mohammad Alsharo'a (Muons, Inc, Batavia), Ivan Gonin, Alfred Moretti, Gennady Romanov (Fermilab, Batavia, Illinois)

Presenter Mohammad Alsharo'a (Muons, Inc, Batavia)

Abstract RF cavities for muon ionization cooling channels can have RF windows over their ends to create better internal voltage profiles and to make them independent of each other. To be effective, the conducting window material must be sufficiently transparent to the muons to not affect the beam cooling, which means low mass and low Z. In the case of pressurized RF cavities, as opposed to those that operate in vacuum, the RF window design is simplified because the heat deposited in the windows from the RF and the beam is carried off by the hydrogen gas. In this report we analyze the thermal, mechanical, and electrical properties of a simple beryllium grid structure to improve the performance of pressurized RF cavities that are to be used for muon beam cooling.

Funding Agency This work was supported in part by DOE STTR grant DE-FG02-02ER86145.

Type of Presentation Poster

ID: 1254 Simultaneous bunching and precooling muon beams with gas-filled RF cavities

Authors Kevin Paul (Muons, Inc, Batavia), David Neuffer (Fermilab, Batavia, Illinois), Yaroslav Derbenev (Jefferson Lab, Newport News, Virginia)

Presenter Kevin Paul (Muons, Inc, Batavia)

Abstract High-gradient, pressurized RF cavities are investigated as a means to improve the capture efficiency, to effect phase rotation to reduce momentum spread, and to reduce the angular divergence of a muon beam. Starting close to the pion production target to take advantage of the short incident proton bunch, a series of pressurized RF cavities imbedded in a strong solenoidal field is used to capture, cool, and bunch the muon beam. We discuss the

anticipated improvements from this approach to the first stage of a muon cooling channel as well as the requirements of the RF cavities needed to provide high gradients while operating in intense magnetic and radiation fields.

Funding Agency This work was supported in part by DOE SBIR grant DE-FG02-03ER83722.

Type of Presentation Poster

ID: 1700 The RF Experimental Program in the Fermilab Muon Test Area

Authors Jim Norem (ANL, Argonne, Illinois), Rikard Sandstrom (CUI, Geneva), Alfred Moretti (Fermilab, Batavia, Illinois), Yagmur Torun (IIT, Chicago, Illinois), Robert Rimmer (Jefferson Lab, Newport News, Virginia), Derun Li, Michael Zisman (LBNL, Berkeley, California), Rolland Johnson (Muons, Inc, Batavia)

Presenter Jim Norem (ANL, Argonne, Illinois)

Abstract The rf R&D program for high gradient, low frequency cavities to be used in muon cooling systems is underway in the Fermilab Muon Test Area. Cavities at 805 and 201 MHz are used for tests of conditioning techniques, surface modification and breakdown studies. This work has the Muon Ionization Cooling Experiment (MICE) as its immediate goal and efficient muon cooling systems for neutrino sources and muon colliders as the long term goal. We study breakdown, and dark current productions under a variety of conditions.

ID: 1352 Design and Expected Performance of the Muon Beamline for the Muon Ionisation Cooling Experiment

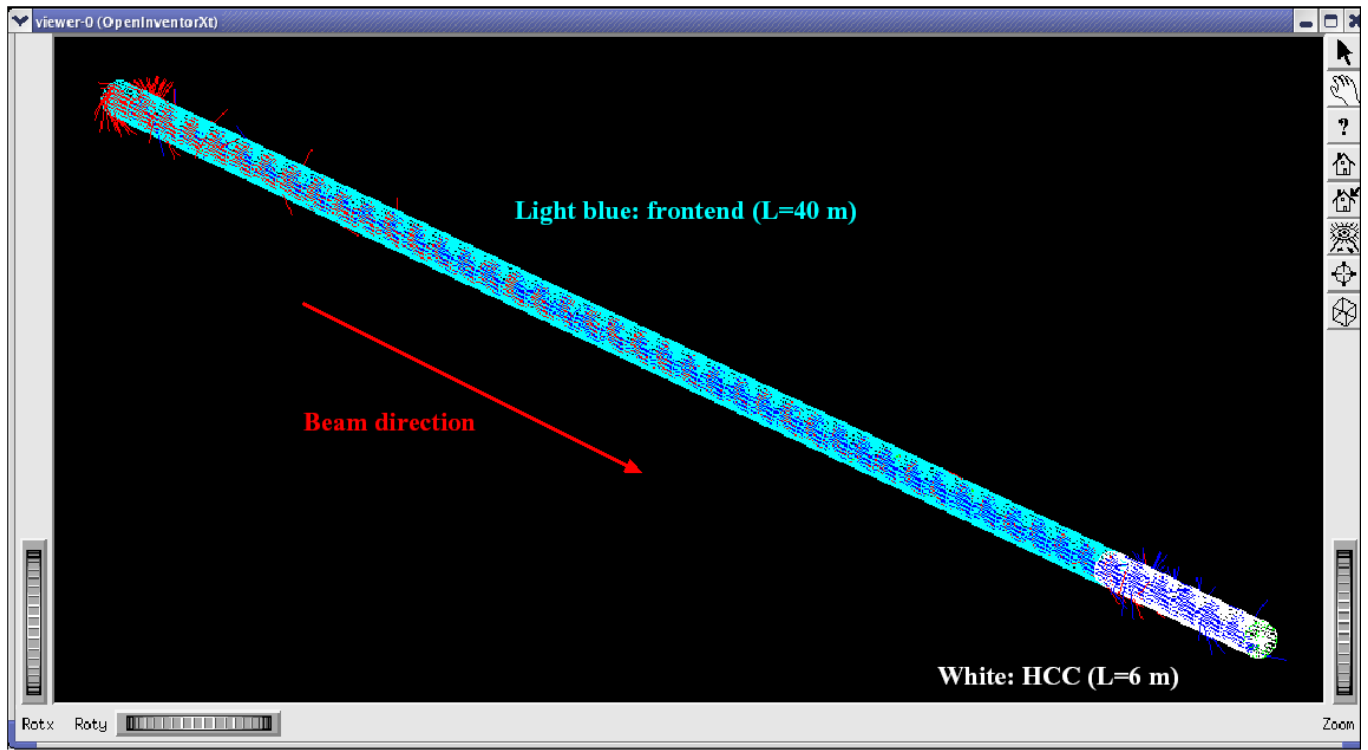
Authors Kevin Tilley (CCLRC/RAL/ISIS, Chilton, Didcot, Oxon), Thomas Roberts (Muons, Inc, Batavia), Kenny Andrew Walaron (University of Glasgow, Glasgow)

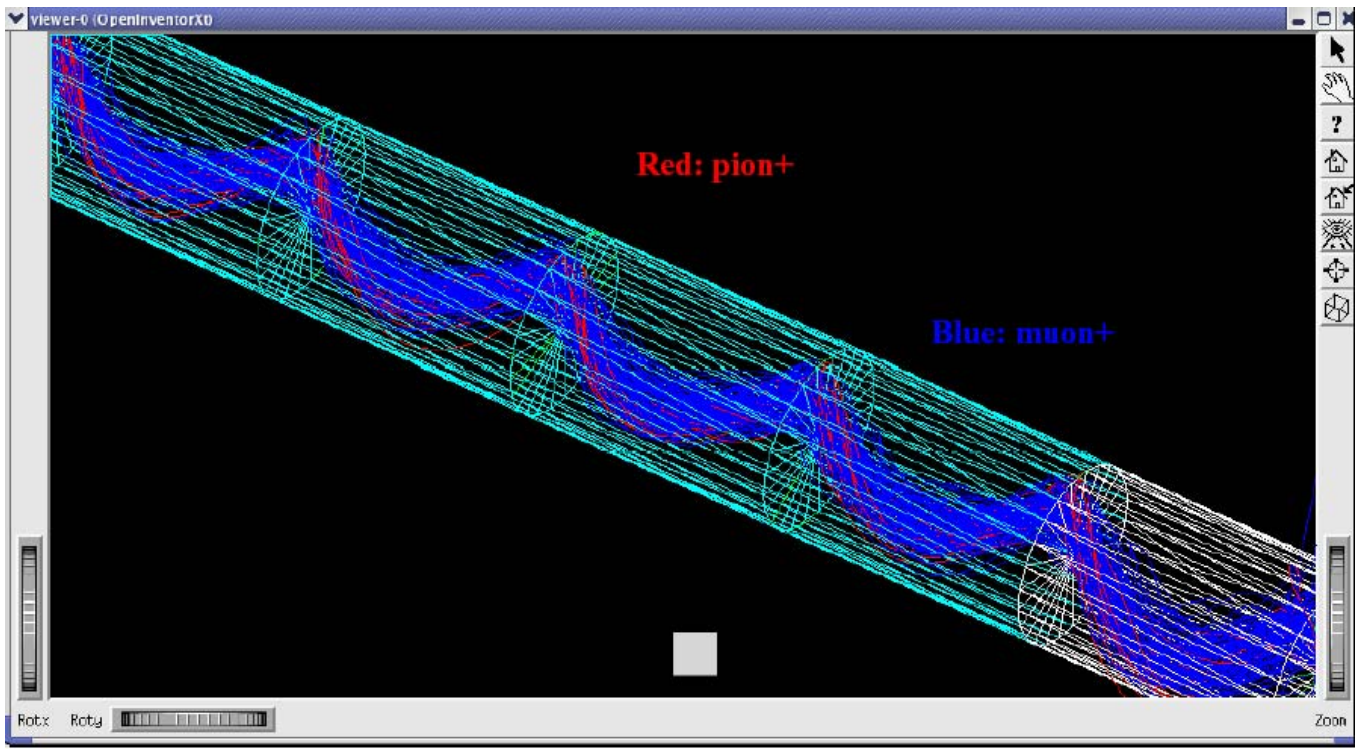
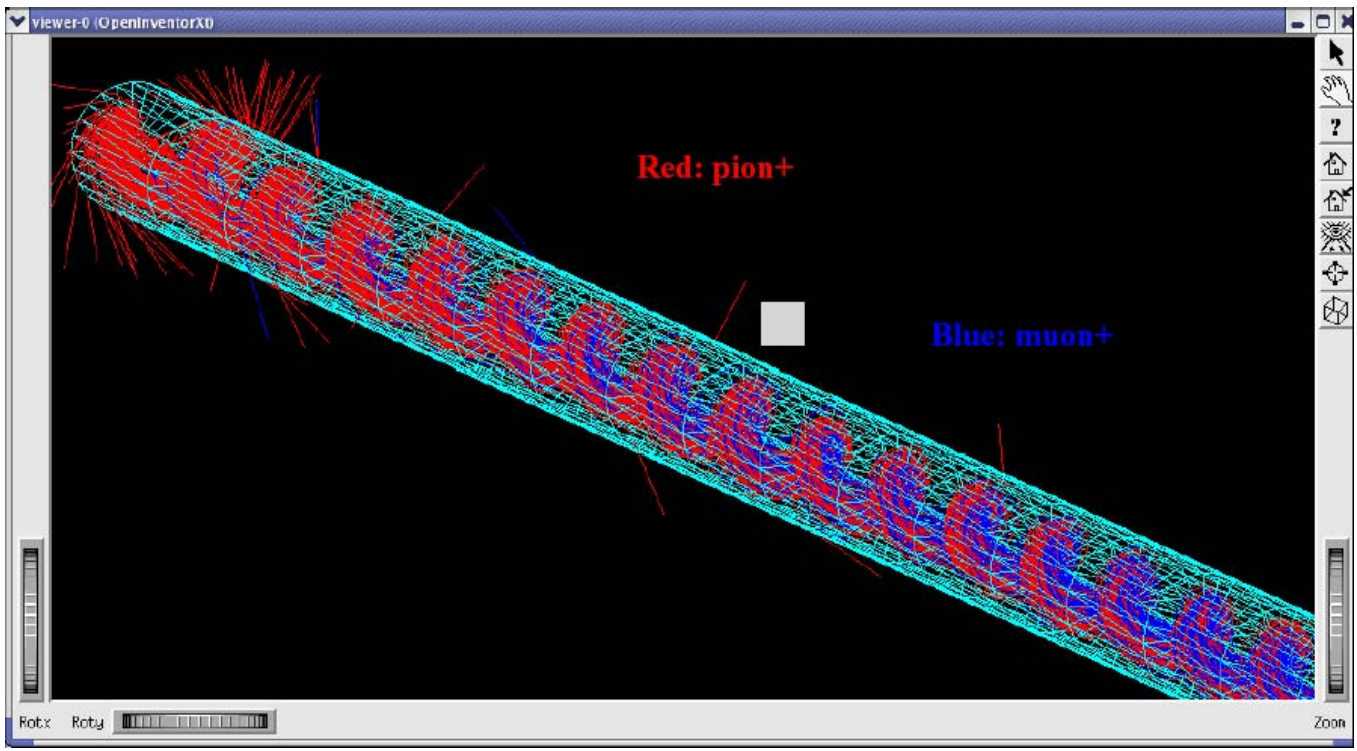
Presenter Kevin Tilley (CCLRC/RAL/ISIS, Chilton, Didcot, Oxon)

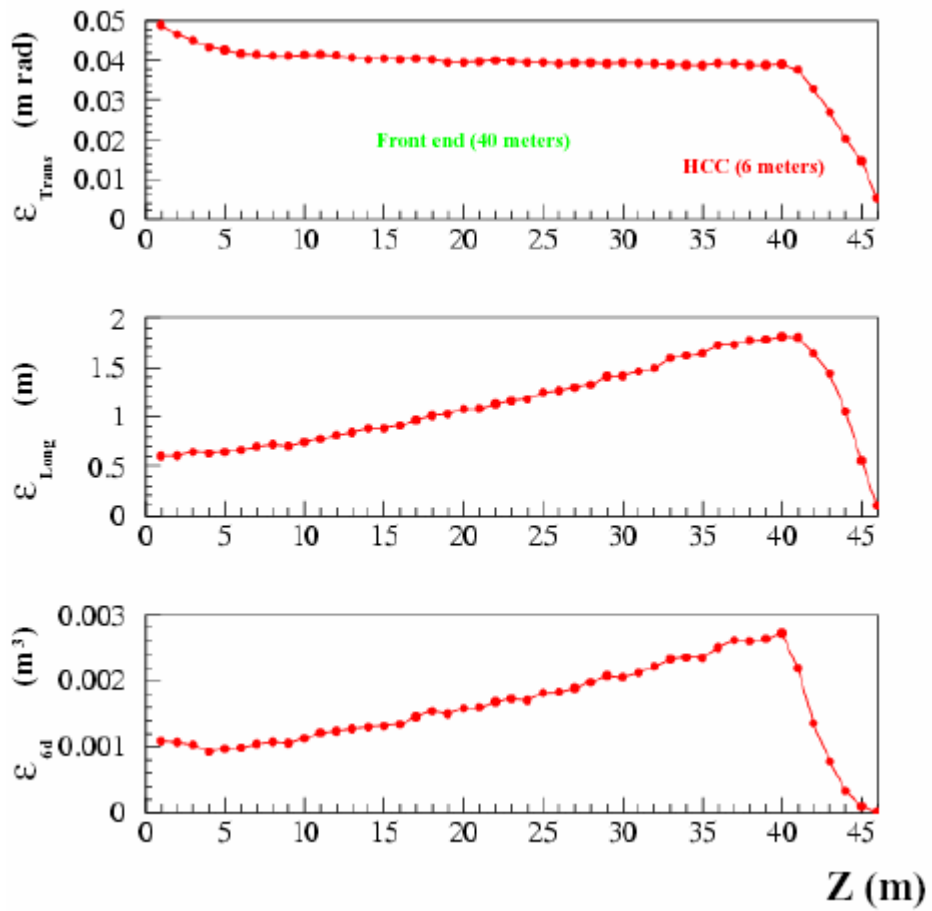
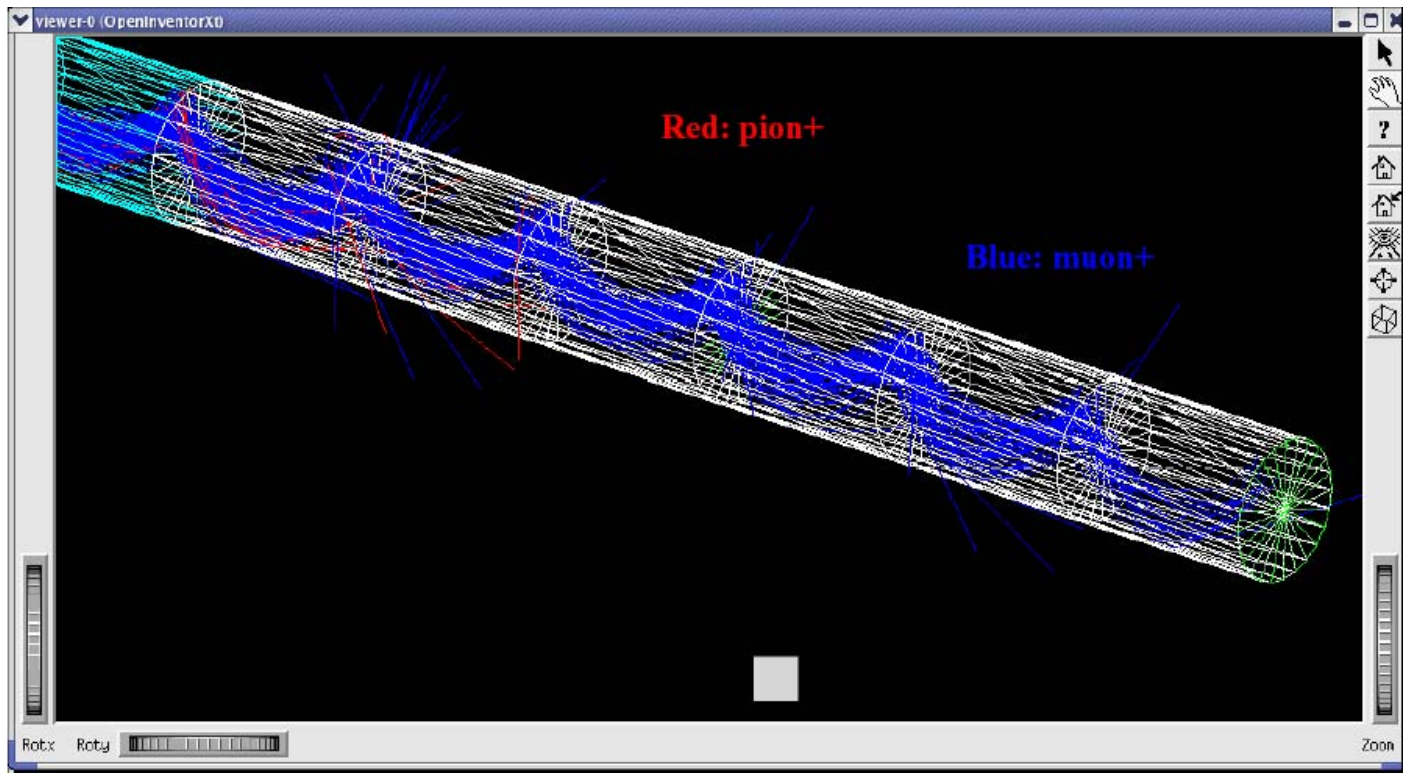
Abstract It is proposed to install a Muon Ionisation Cooling Experiment (MICE) at the ISIS facility, at Rutherford Appleton Laboratory (RAL). This experiment will be the first demonstration of ionisation cooling as a means to reduce the large transverse emittance of the muon beam, produced during the early stages of a Neutrino Factory. In order to permit a realistic demonstration of cooling, a beam of muons must be produced, possessing particular qualities, notably in emittance and momenta. This paper describes the current design for the muon beamline, outlining issues particular to the needs of the MICE experiment, and discusses its expected performance.

Appendix IV – First pion decay and muon pre-cooler HCC simulation

Attached pdf file shows the simulation result by using the helix channel as the frontend and following with the non-rf HCC. This is a first result. There are many things to improve this design. 5,000 pions are injected from one end and the number of good particles at 40 meters (which corresponds to the end of the frontend) are around 3,000. Immediately after, those particles inject into the non-rf HCC, then the number of good particles at the end of the designed field in the HCC ($z=44$ meters) is 1,500. So the transmission efficiency is $\sim 50\%$. I did not take into account the number of rest pion at the end of channel. So this number can be bigger. The cooling factor in the transverse and longitudinal directions are slightly less than 2. Then the 6D cooling factor reaches around 8. The figure merit is, therefore, around 4. The reference particle in the frontend channel is a 470 MeV/c pion⁺. Therefore, the field strength is slightly higher than those at the one end of the HCC. There could be a mismatching. But I believe that we can significantly reduce this problem by using the series of the helix channel. The assumptions of this design are 1). the spacial distribution of produced pions from just after an inner target can be small ($dx, dy = \pm 20$ mm) since the frontend channel can be installed immediately after the pion production point, 2). The momentum deviation of the production pion is 470 MeV/c \pm 50 MeV/c. Again, this is just a first result. I did not tune the field parameters precisely. I will study about this if you want. Please let me know.







Appendix V – MANX design

Preliminary Simulation Results for a 5 m long 6D HCC MANX section are shown in Figure 3. In this simulation, 400 MeV/c muons are degraded to less than 200 MeV/c in making 5 turns in the HCC filled with liquid hydrogen.

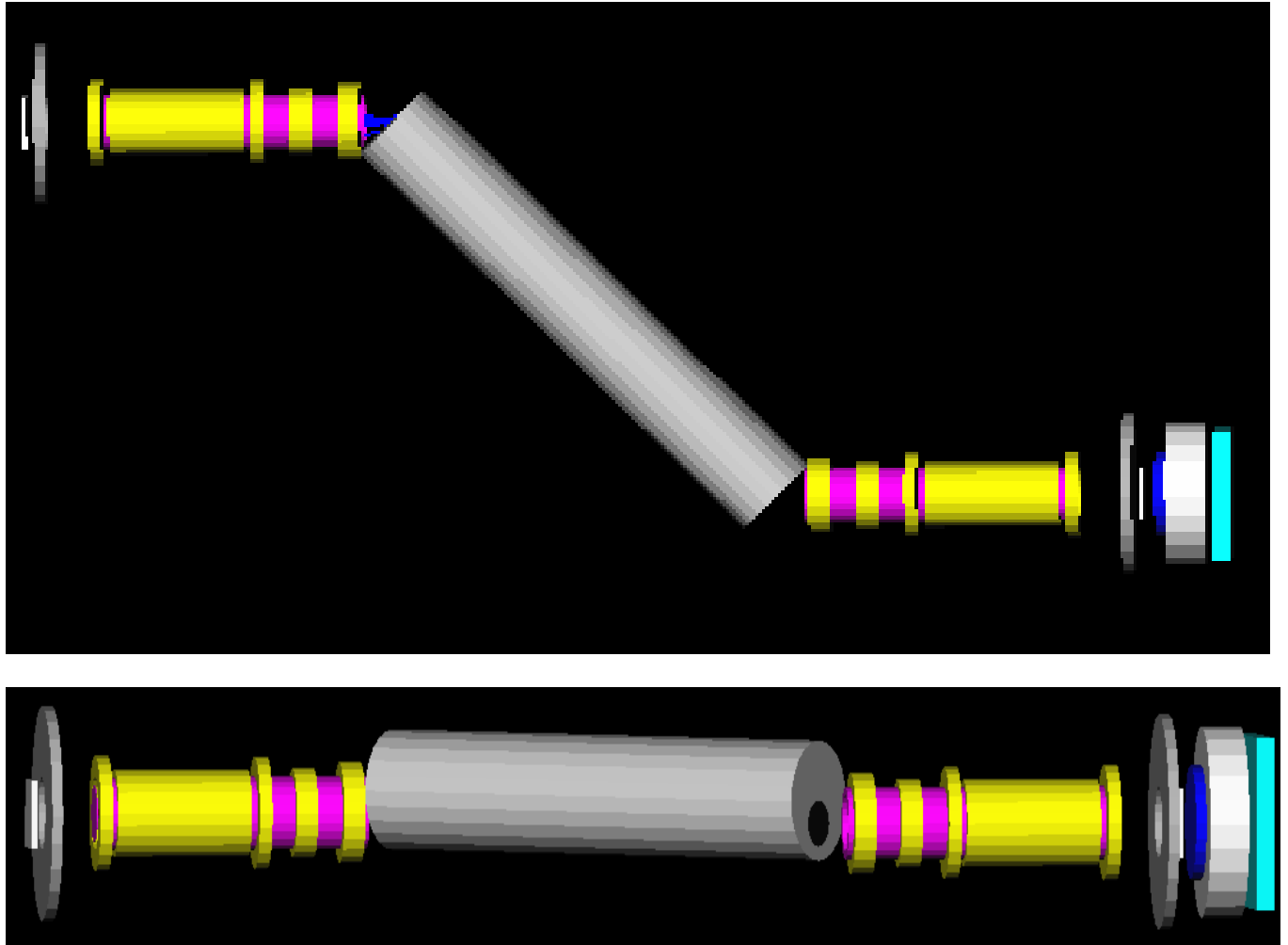


Fig. 2. G4BL simulation program displays of the plan (upper) and elevation (lower) views of the MANX HCC using the particle identification devices of MICE. The yellow devices correspond to the matching coils and spectrometer magnets of the particle measurement sections of the MICE experiment shown in Figure 1. The gray cylinder is the HCC that is the heart of MANX and represents the cryostat that is the subject of this proposal.

A conceptual picture of the 6D MANX is shown in figure 2. The gray cylinder represents the HCC, which is the new device to be built. It is a solenoid with transverse helical dipole and quadrupole magnets that is filled with liquid hydrogen. Muons enter from the left of the picture and pass through the (yellow) solenoidal spectrometer section instrumented with scintillating fiber detectors. The muons then enter the HCC at a horizontal angle and vertical offset to match

onto the equilibrium orbit. In terms of the equations above, $\kappa \equiv ka = p_{\perp} / p_z = 1$, the helix pitch angle and beam entrance angle is 45 degrees, and the helix period $\lambda = 1$ m, giving a radial offset $a = 1/2\pi = 15.9$ cm. The equilibrium orbit then follows a helical path with 5 turns in the HCC before exiting into the downstream spectrometer system. There are two 32 cm diameter liquid hydrogen containment windows at each end of the HCC, where the downstream window is seen as a black ellipse on the end of the gray cylinder in the figure.

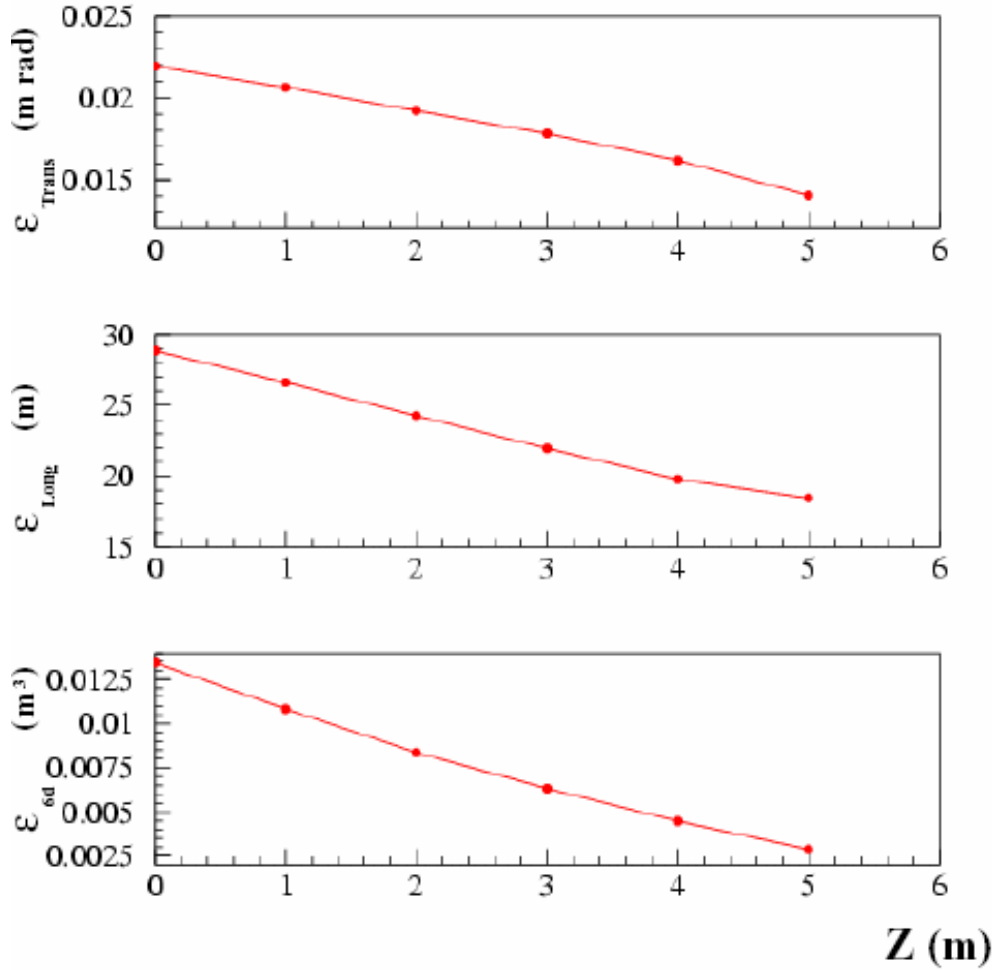


Fig. 3. Simulation results for a 5 m HCC filled with liquid hydrogen.

Figure 3 shows the normalized transverse (only one transverse plot shown), longitudinal, and 6D emittances plotted as a function of the distance down the channel. The settings of the helical dipole and quadrupole magnets and the solenoid are chosen to give equal cooling decrements in all three planes. The combined 6D cooling factor is about 5.4, corresponding to 1.7 coming from each of the three planes. The improved performance this MANX simulation relative to the MICE design (which has a cooling factor close to 1.1 or a 10% effect and no longitudinal cooling) comes from the effectiveness of HCC, from the greater path length in the hydrogen absorber ($5 / \cos(45^\circ) = 7.07$ m), and from the effects of the high-Z windows. MICE has several

aluminum windows for hydrogen containment and separation from the RF cavities, while the two windows needed for MANX have not yet been included in the simulation.

Appendix VI – First HCC ANSYS Studies

Case 1. Natural Convection Analysis of RF Cavities Pressurized with GH₂

Cavity geometry: Two-dimensional cavity model (circle) is assumed to simplify the calculations and reduce the computation time. The radius of the circle is chosen to be 13.48 cm so that the frequency of the cavity, filled with hydrogen gas at 77K and 1600 psi, is 805 MHz.

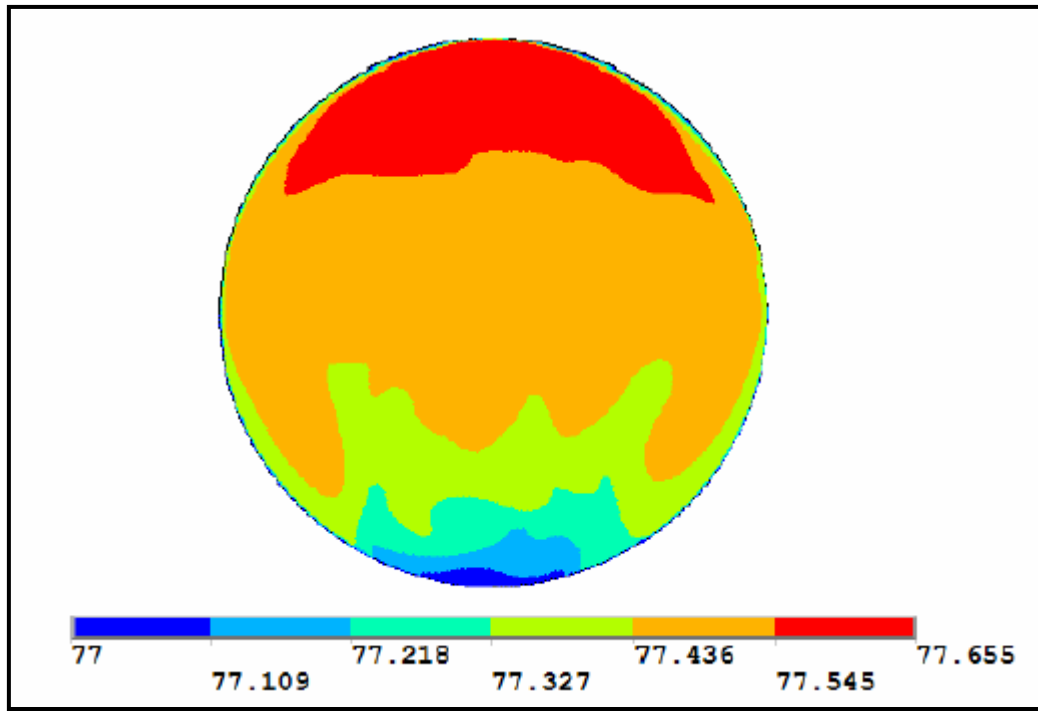
Natural convection is assumed, where the initial velocity of the gas is zero. - Steady and unsteady solution is obtained. Temperature of the internal side of the cavity is assumed to be 77 K. Initial gas Pressure = 1600 psi, Initial gas temperature =77K. Software used: ANSYS FORTRAN.

FEA model verification: comparing the current results with the LH2 absorber convection results.
 $dE/dX=22.325 \text{ [MeV/m.particle]} = 22.325 \cdot 10^6 \cdot 1.6 \cdot 10^{-19} = 35.72 \cdot 10^{-13} \text{ [J/m.particle]}$

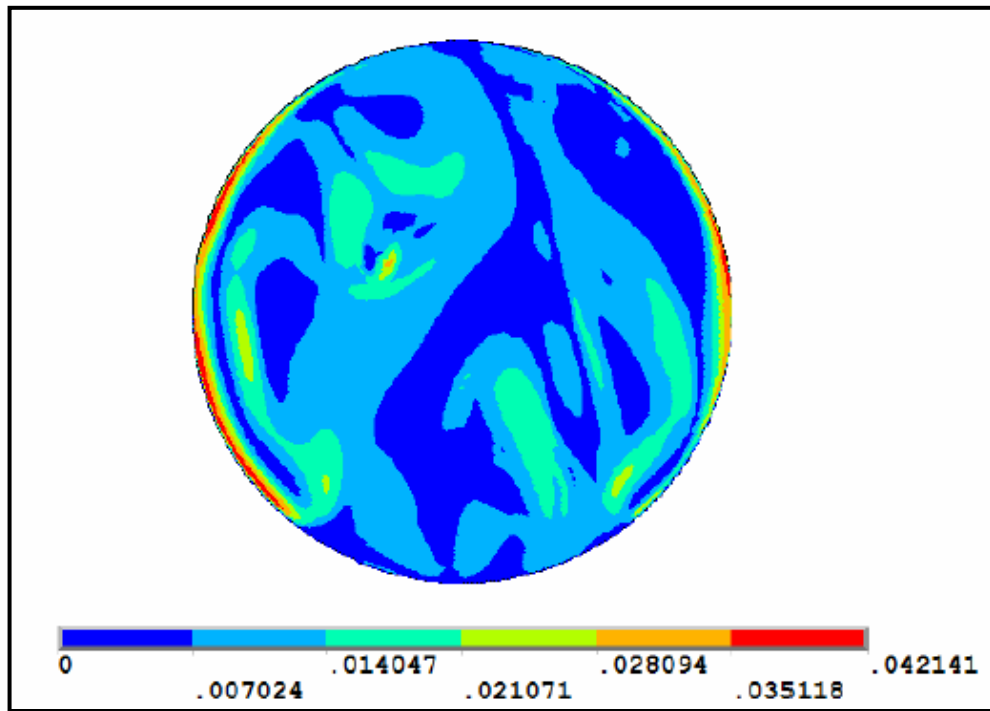
Heat Input = $35.72 \cdot 10^{-13} \text{ [J/m.particle]} \cdot 10^{13} \text{ [particles/pulse]} \cdot 5 \text{ [pulse/sec]} = 178.6 \text{ W/m}$

Parameter	Value
Reference Temperature (K)	77
Reference pressure (MPa)	11.03
Density (kg/m ³)	34.733
g (m/s ²)	9.81
Viscosity (kg/m-s)	5.47E-06
Kinematic viscosity (m ² /s)	1.58E-07
Specific Heat (J/kg-K)	1.55E+04
Thermal conductivity (W/m-K)	0.098
Thermal diffusivity (m ² /s)	1.82E-07
Coefficient of thermal expansion (1/K)	0.012987013
Radius of the cavity (m)	0.1348
Heat Generation per unit length (W/m)	178.6
Heat Generation per cupic length (W/m ³)	3128.612654
Heat Generation Profile	Uniform
Pr	0.865227143
Ra	2.02E+14
Nu	167.9
h (W/m ² -k)	61.03
Temperature-non dimensional	5.17E-04
Temperature rise (K)	1.115

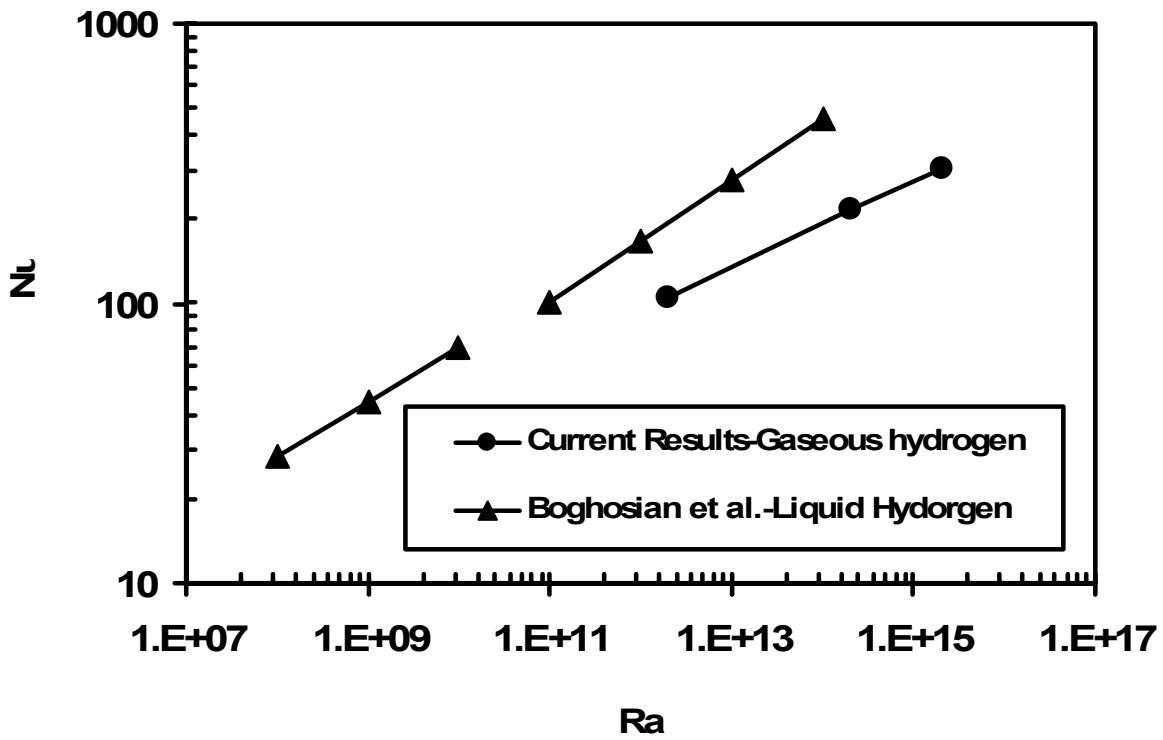
$$Ra = \frac{g \beta q'' D^5 \rho c_p}{K^2 \nu} \cdot \frac{1}{T_{nond}} \cdot \frac{1}{q'' D^2 / K} \cdot \frac{1}{Nu} \cdot \frac{1}{K}$$



Contour plot of temperature (K)



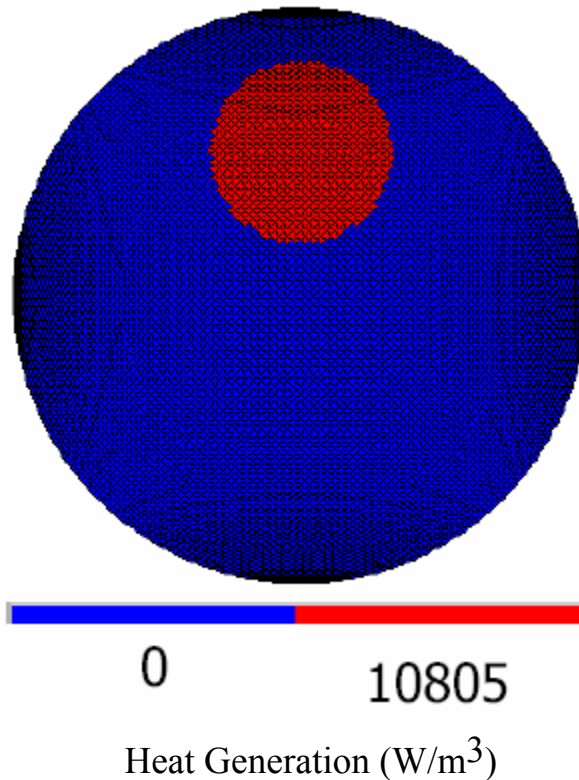
Contour plot of magnitude of velocity (m/sec)



Case 2. Natural Convection Analysis of MANX LH₂ Energy Absorber

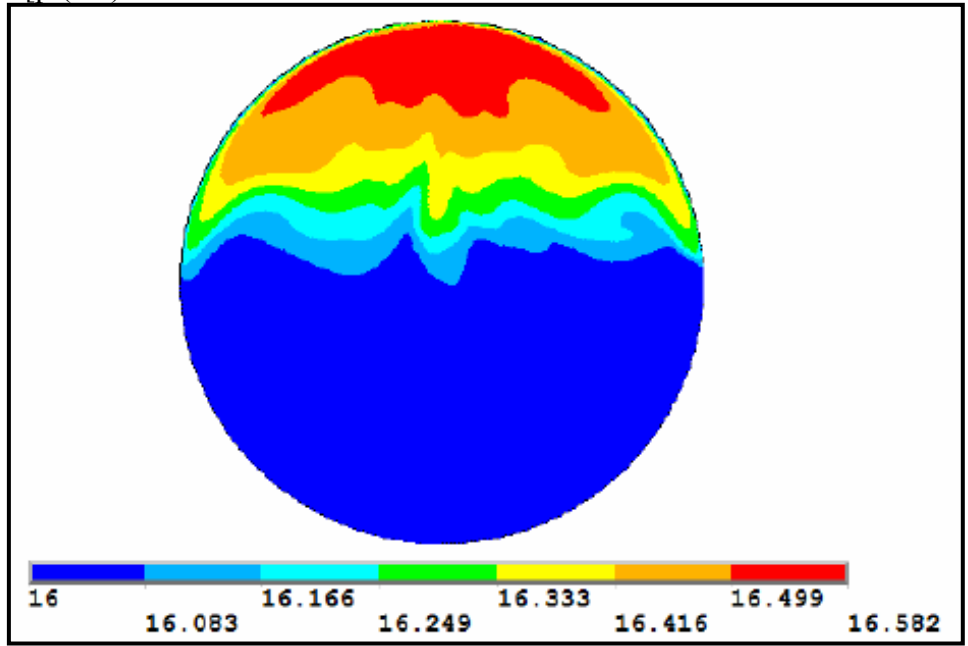
Parameter	Value
Reference Temperature (K)	16
Reference pressure (MPa)	0.15
Density (kg/m ³)	75.2472
g (m/s ²)	9.81
Viscosity (kg/m-s)	1.96E-05
Kinematic viscosity (m ² /s)	2.61E-07
Specific Heat (J/kg-K)	7.42E+03
Thermal conductivity (W/m-K)	8.91E-02
Thermal diffusivity (m ² /s)	1.60E-07
Coefficient of thermal expansion (1/K)	1.21E-02
Diameter of the channel (m)	0.64
Heat Generation per unit length (W/m)	3394.4
Heat Generation per cubic length (W/m ³)	10,804.70
Heat Generation Profile	Shifted Beam
Beam Profile	Circle-DIA = 20cm, offset=16cm
Pr	1.635708076
Ra	3.73E+16
Temperature-non dimensional	1.96E-06
Temperature rise (K)	0.58

Analysis parameters and gas thermal properties

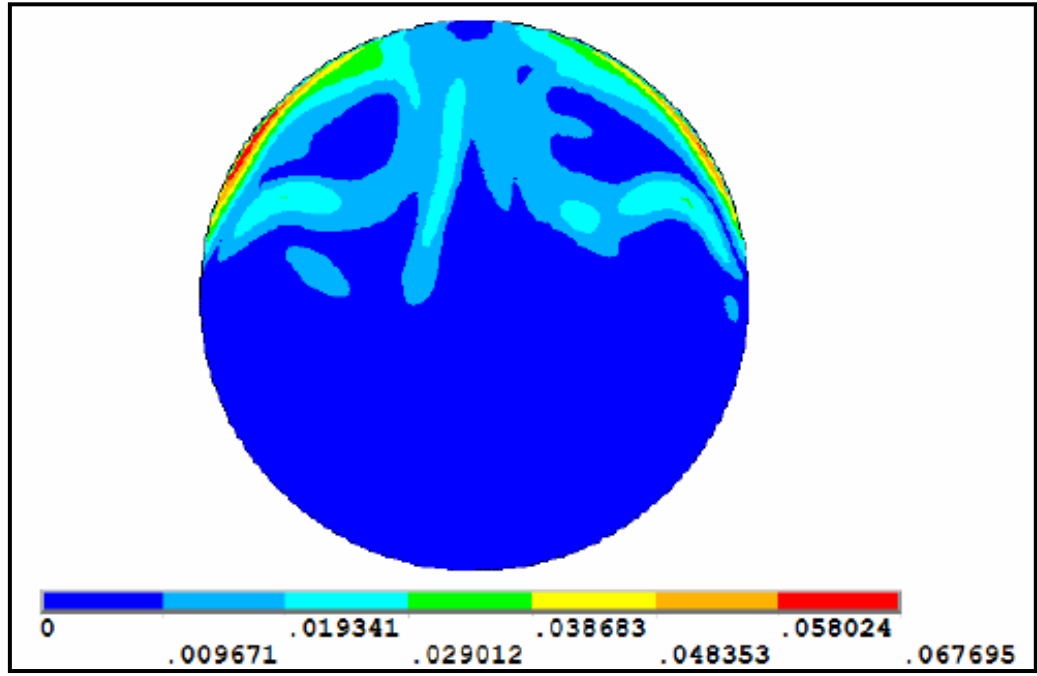


$$q' = 42.43 \times 10^6 \text{ eV/m} \times 10^{14} \text{ particles/pulse} \times 5 \text{ pulse/sec} \times 1.6 \times 10^{-19} \text{ J/eV} = 3394.4 \text{ W/m}$$

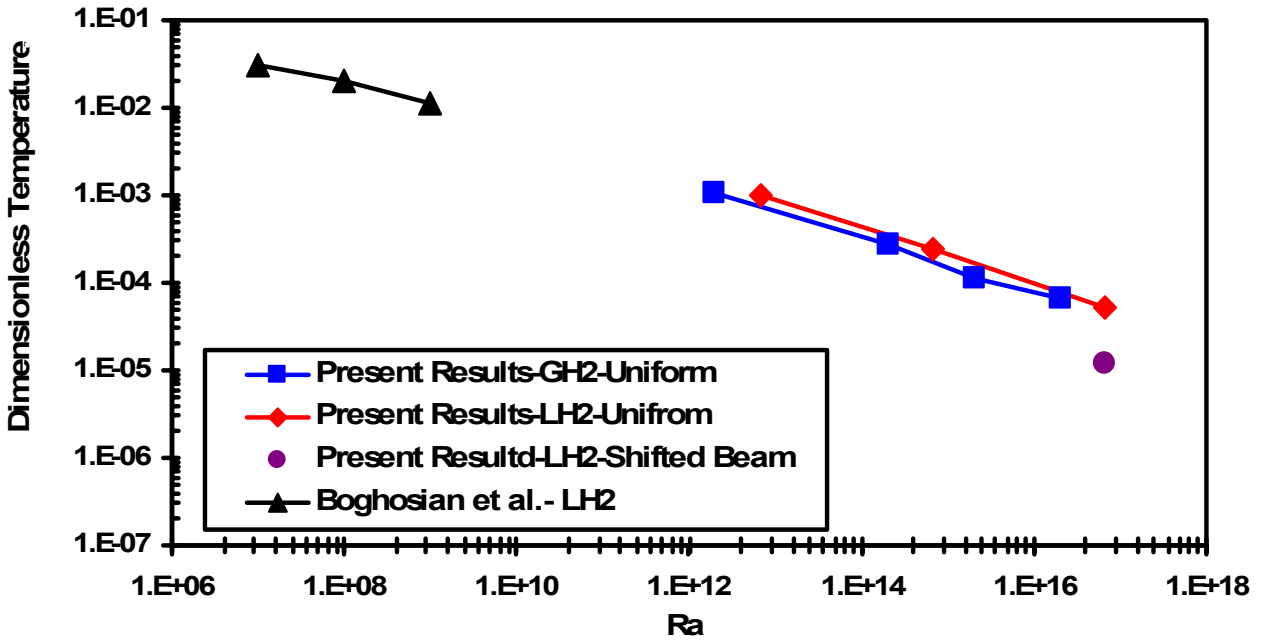
$$q''' = 3394.4 / [\pi(0.1)^2] = 10805 \text{ W/m}^3$$



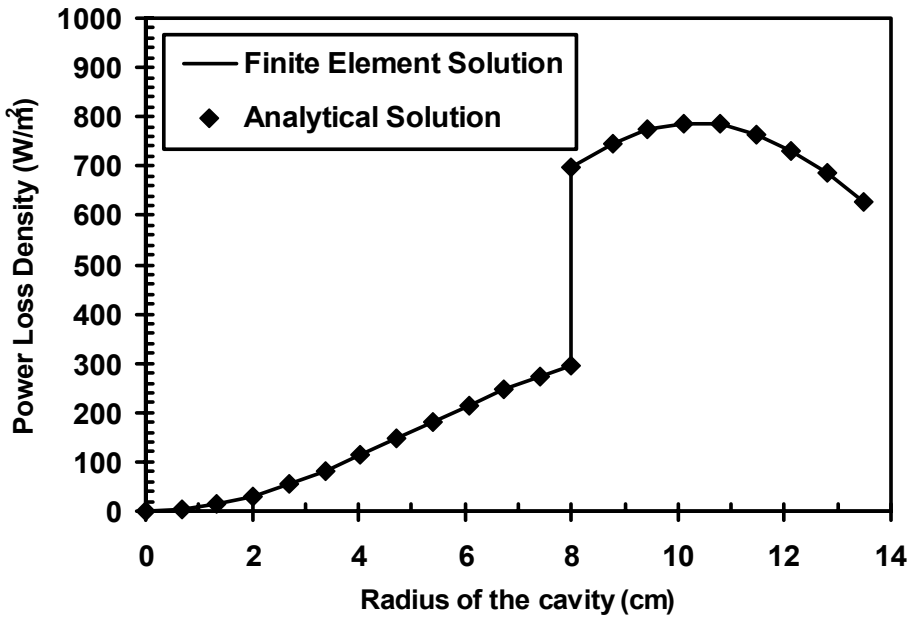
Contour plot of temperature (K)



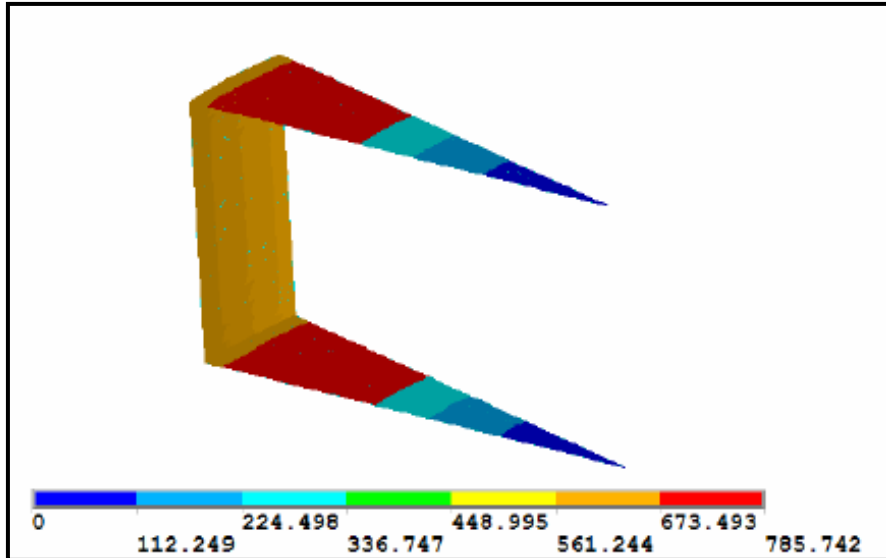
Contour plot of magnitude of velocity (m/sec)



Case 3. Thermal Analyses of an RF cavity Pressurized with Hydrogen Gas.



Power loss density profile

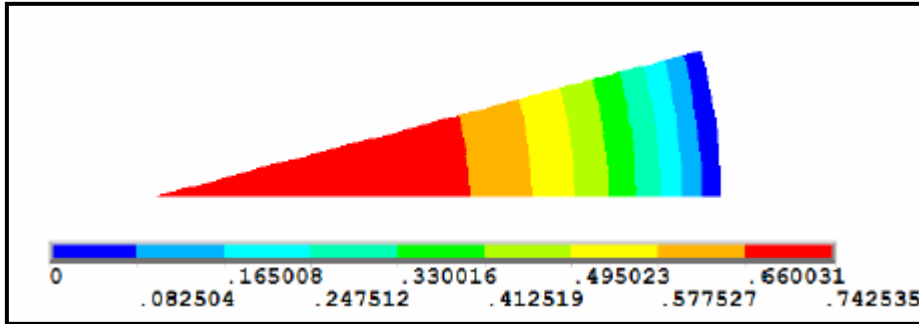


Contour plot of the Power loss density (W/m^2)

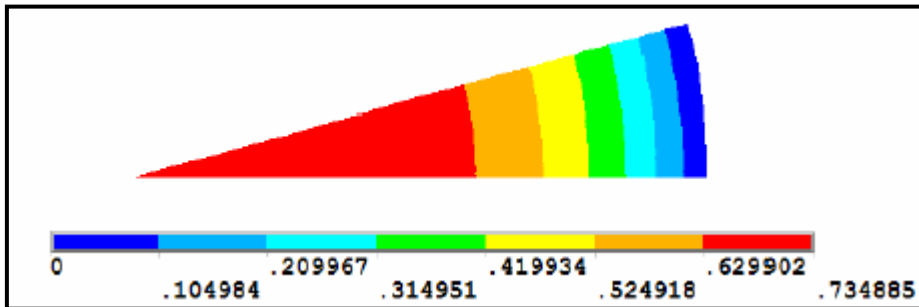
	Vacuum	HP CAV 77K	Rel. Difference
Quality Fcator	20260.894	65389.87	222.74%
Tot .P Loss (w)	333.24	103.2448	-69.02%

Comparison of quality factor and total power loss between an 805 MHz pillbox vacuum cavity and an 805 MHz pillbox cavity pressurized with GH2 at 77K, 1600 psi.

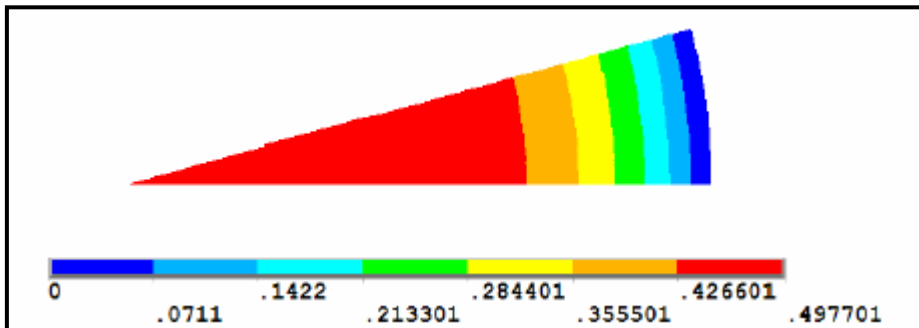
Case 4. Contour plot of the temperature rise distribution in a beryllium window of thickness of 127 microns.



RF, No flow, and no beam

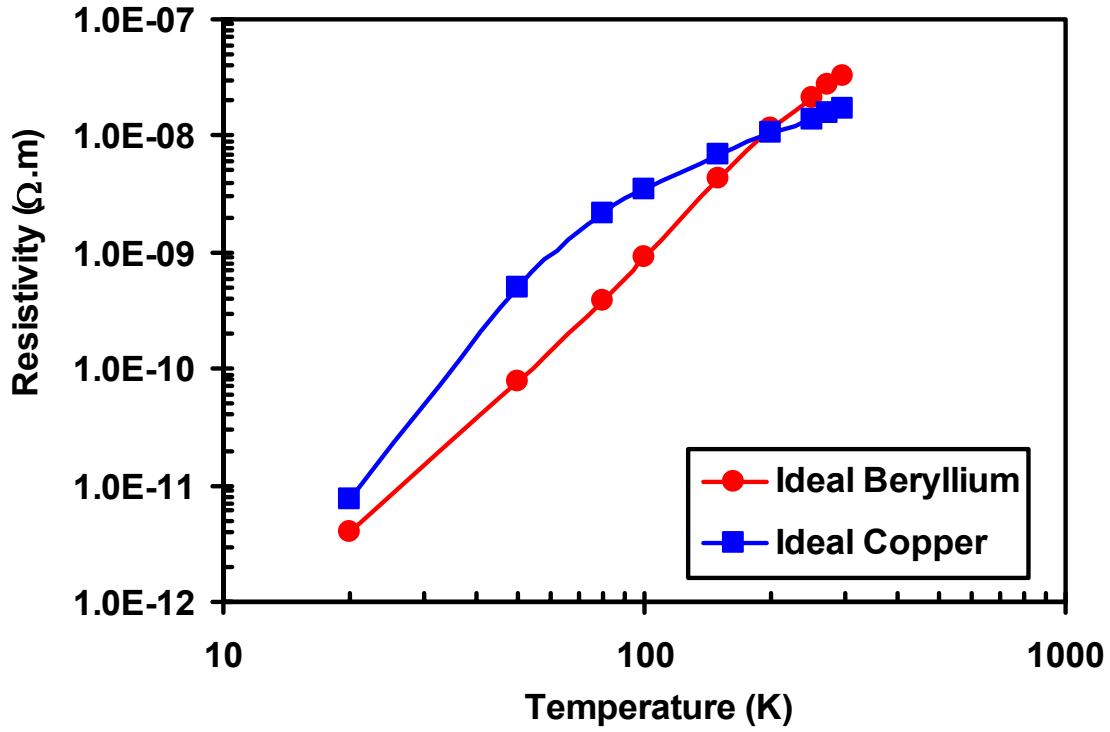


RF, GH₂ Flow (77K, 1600 psi), but no beam



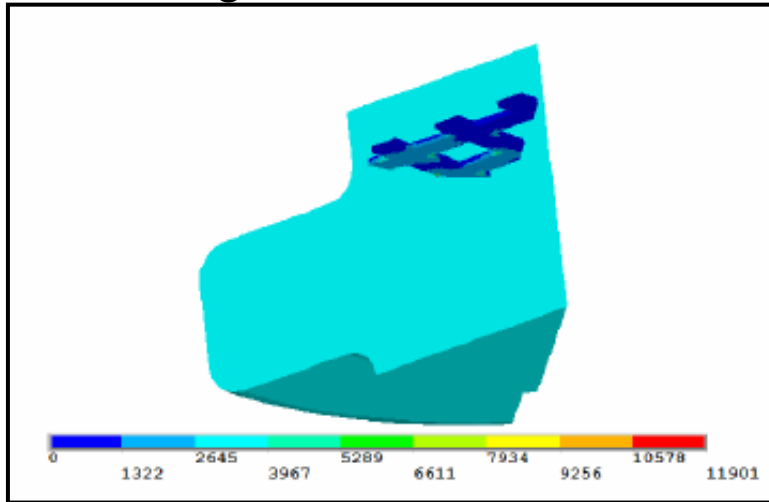
RF, GH₂ Flow (77K, 1600 psi), and beam (Ra=2.02e14)

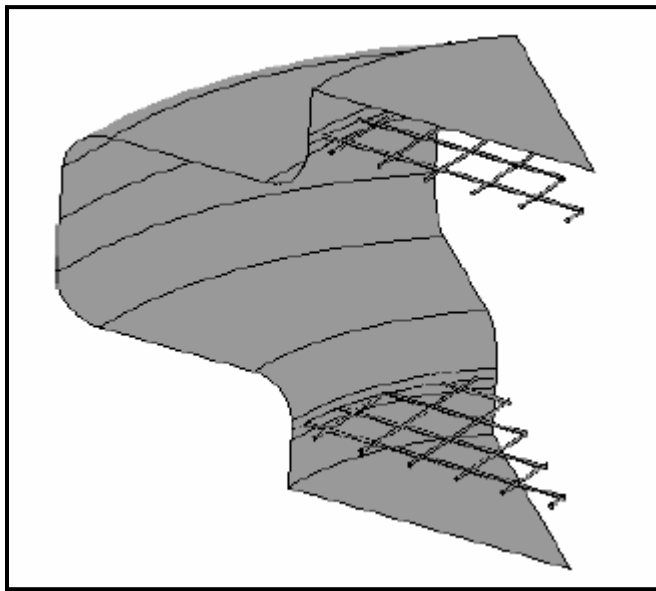
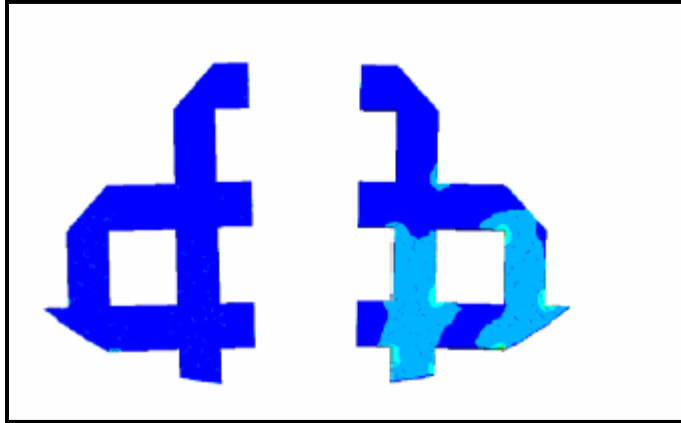
Case 5. Electromagnetic Analysis of Beryllium RF Cavities



Resistivity .vs. Temperature curves

Case 6. Studies of Be grids for Pressurized RF Cavities



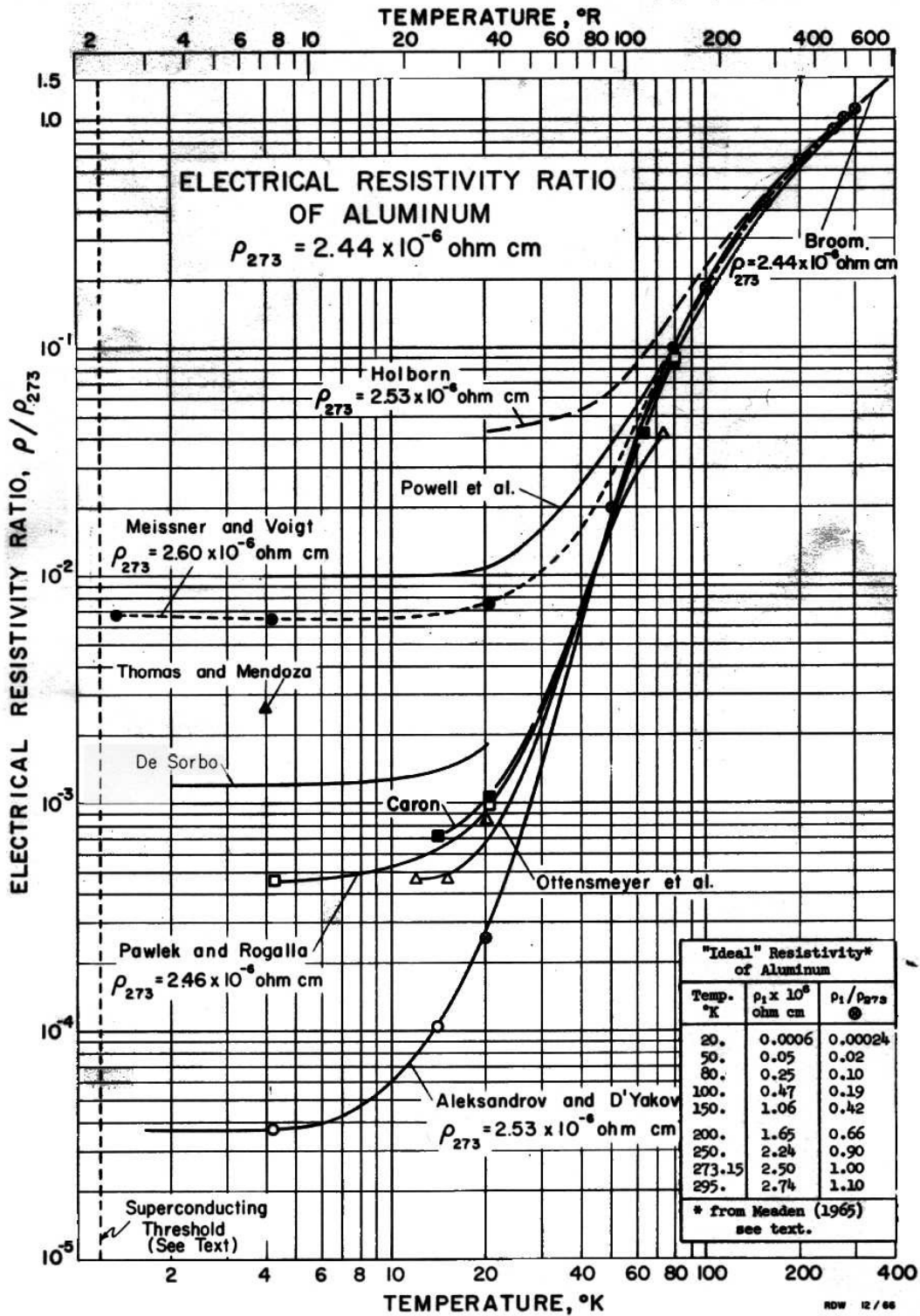


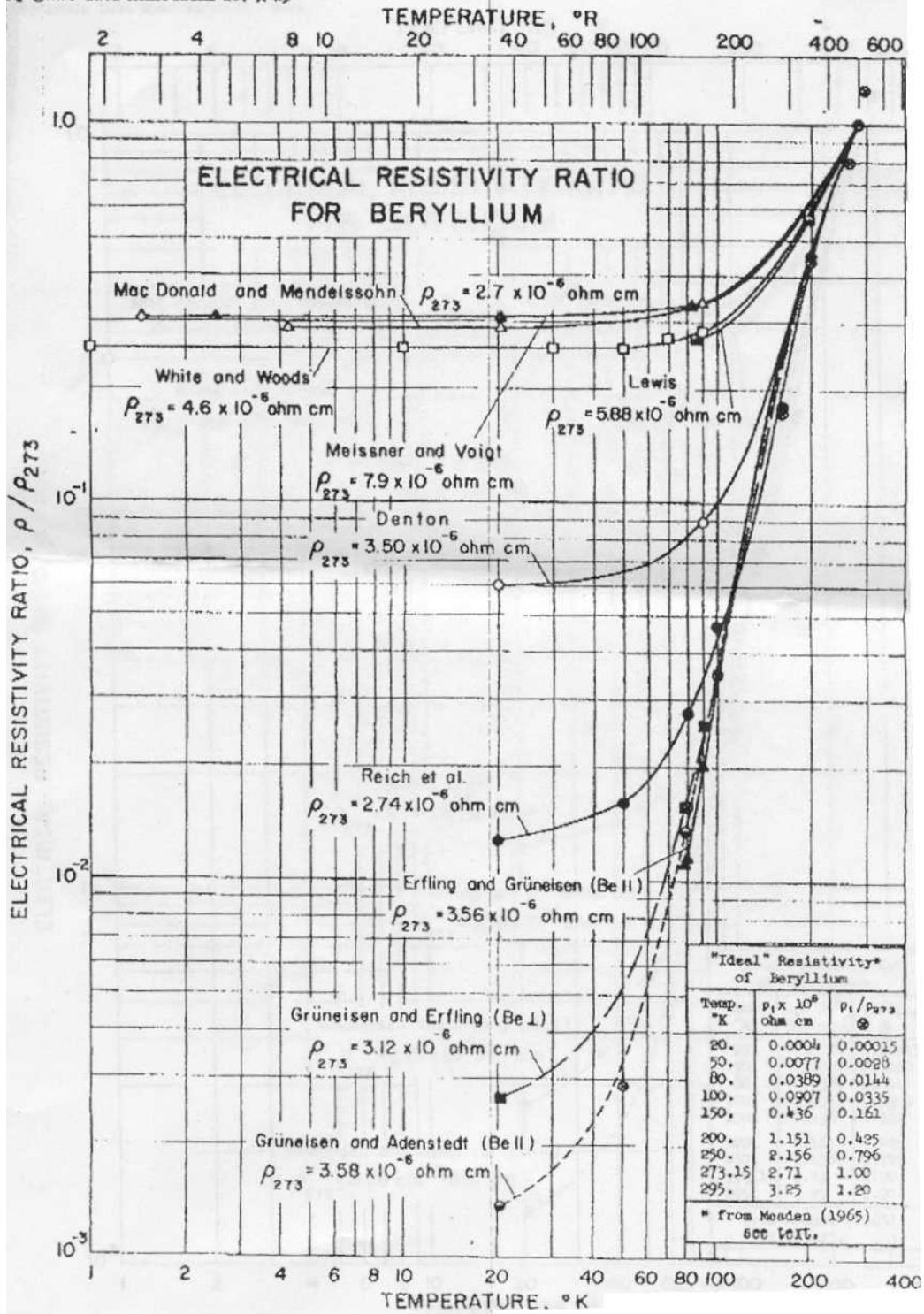
Which grid option should we use for the current proposals?

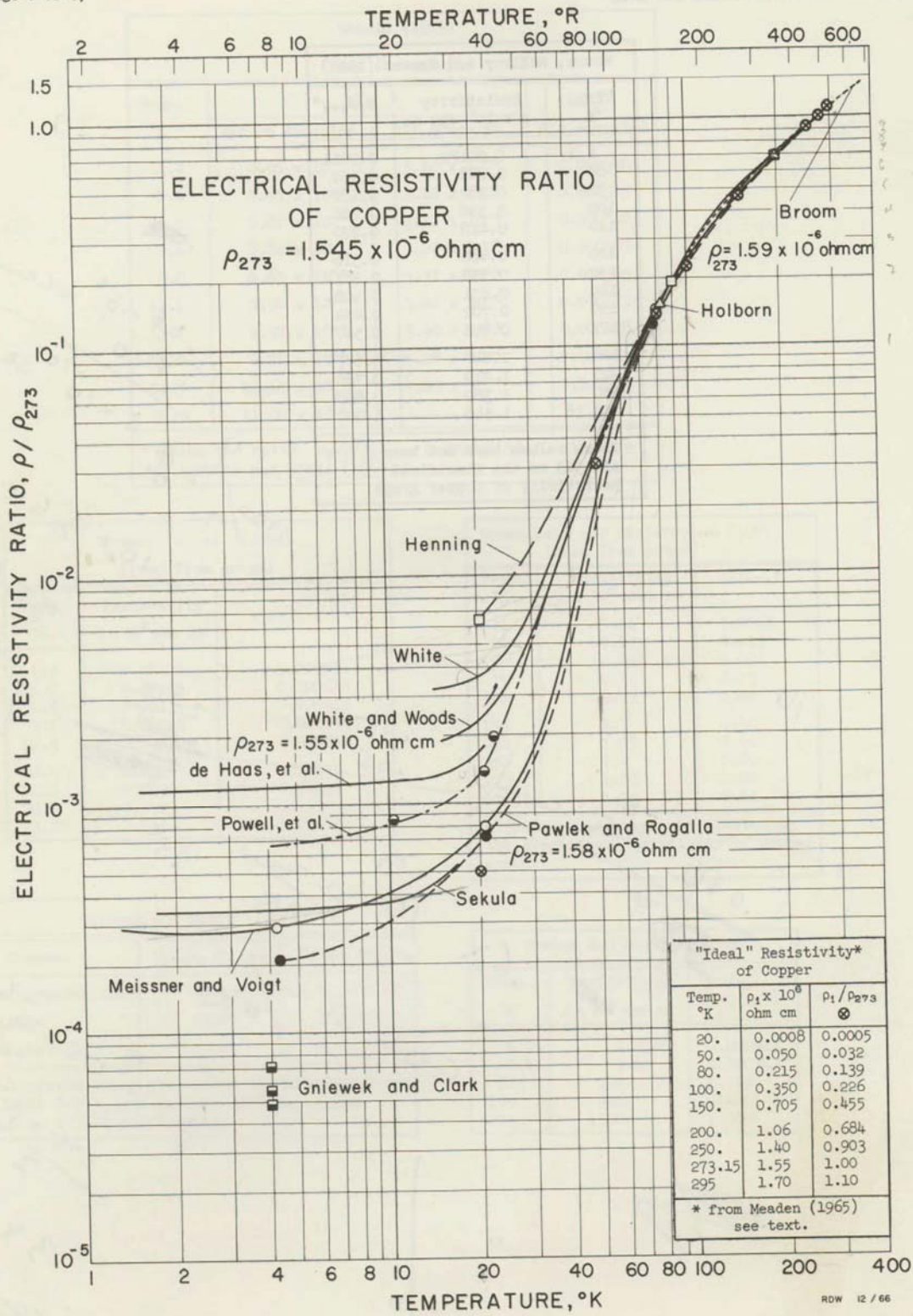
Appendix VII – Resistivity vs T

(page 8 of 8)

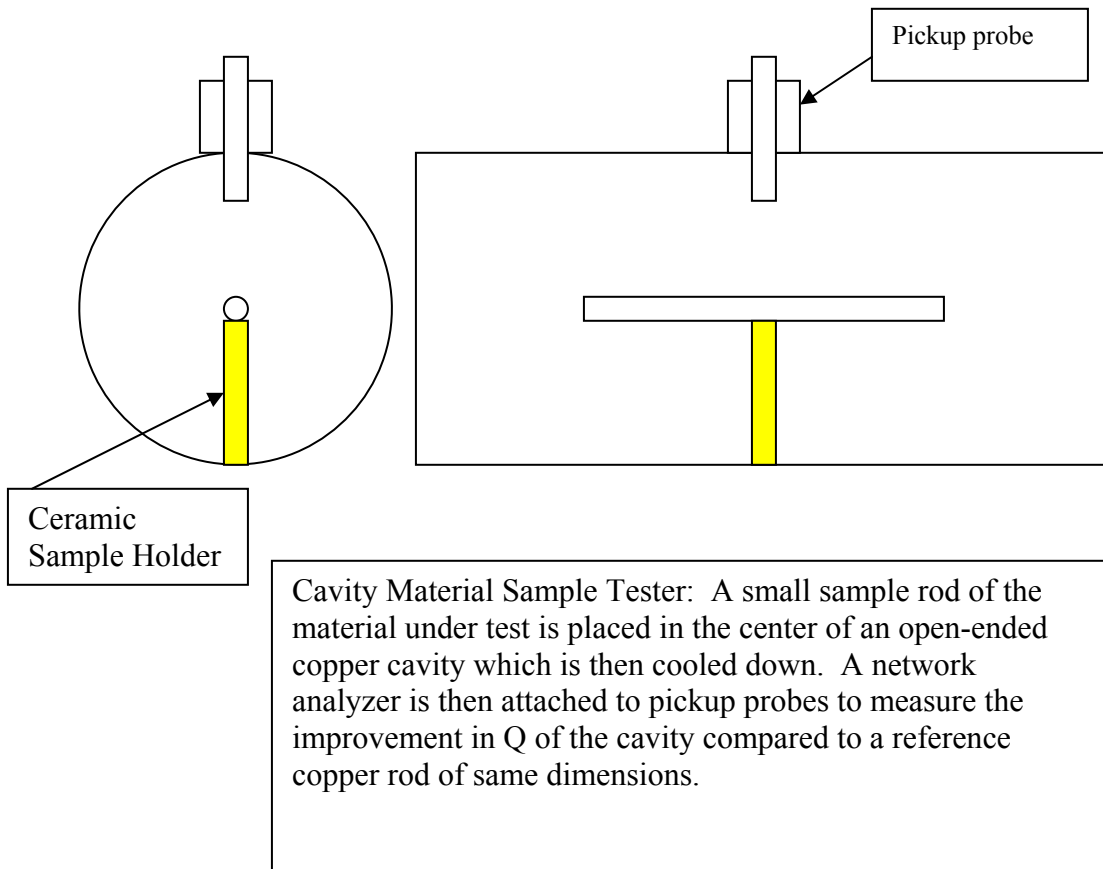
Electrical Resistivity of Aluminum
Cryogenic Data Memorandum No. M-9







Appendix VIII – Resistivity Measurement Schematic



The above figure shows the sample cavity tester. The outside cylinder of the cavity is made of 3 inch diameter OFHC copper. Small sample rods of the materials under test are placed in the center portion of the cavity supported on a very low loss ceramic standoff. The ends can be open to allow the free flow of coolant. All measurements are referenced to an OFHC copper reference sample with identical dimensions as the test sample. After measurements at various temperatures, the reference and sample rods will be cut to shorter lengths to allow measurements at higher RF frequencies.

Materials to be tested are: High purity solid Be rods; various grade of solid Be rods; sputtered Be on substrates of different material, ceramics, metals; electroplated and evaporated Be on different material substrates. Other materials include various grades of Aluminum and Copper in similar configurations.

These measurements will be used to determine the best and most economical metals for constructing of RF cavities to take advantage of their fast resistivity drop off with temperature. In parallel, the studies of breakdown of metals in dense gases and in high magnetic and radiation fields will tell us which of the choices is most appropriate for the conditions of interest.

Appendix IX – HTS data from this Grant
**TESTING OF BSCCO WIRES FOR HIGH TEMPERATURE
SUPERCONDUCTING MAGNETS**

Introduction

High temperature superconductors (HTS) are being considered for the superconducting magnets to be used in the Helical Cooling Channel (HCC) of this proposal. An example of HTS crystal structure is given in Fig. 1 for $\text{Bi}_2\text{Sr}_2\text{CaCu}_2\text{O}_8$ (BSCCO-2212). The current is carried by the copper oxide layers shown in the figure.

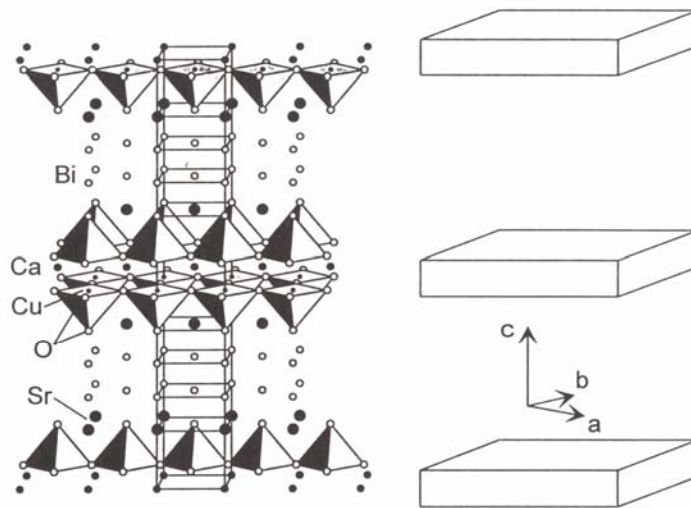


Fig. 1. Crystal structure of $\text{Bi}_2\text{Sr}_2\text{CaCu}_2\text{O}_8$.

BSCCO conductors are typically produced in the form of tapes and, more recently, of round wires. Fig. 2 shows the geometrical configuration of a tape and relative directions of magnetic field. The longitudinal direction is along the length of the tape. The transverse direction, orthogonal to the length of the tape, which is parallel to the tape width, is also called "ab-trans" or "lateral" or "long transverse". The transverse direction, orthogonal to the length of the tape, which is perpendicular to the tape face, is also called "c-axis" or "normal" or "short transverse". Magnetic fields having longitudinal or long transverse directions are both parallel to the tape surface. A magnetic field having short transverse direction is perpendicular to the tape surface.

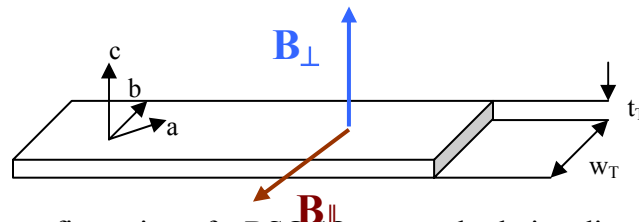


Fig. 2. Geometrical configuration of a BSCCO tape and relative directions of magnetic field.

A comparison of the performance at 4.2 K of state-of-the-art HTS materials is shown in Fig. 3, where the engineering critical current density, J_E , is plotted as a function of magnetic field. The J_E is calculated over the entire cross section of the wire.

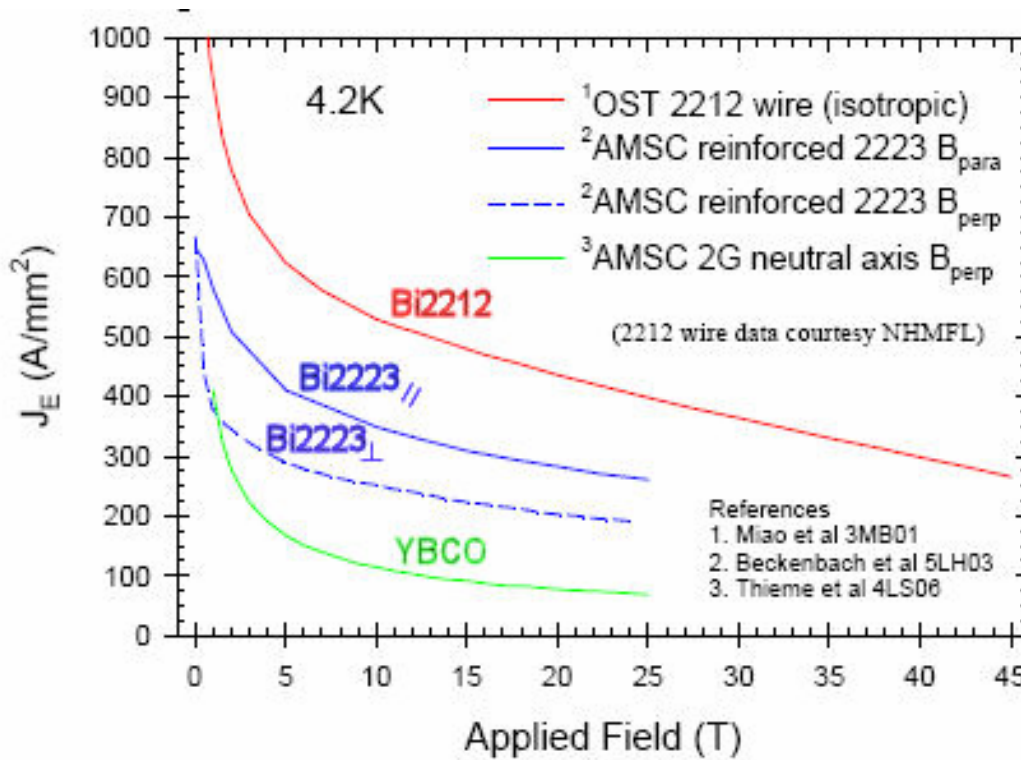


Fig. 3. The engineering critical current density, J_E , at 4.2 K as a function of magnetic field for various HTS materials.

First results

The first conductor that was considered and tested for this proposal is the High Strength BSCCO-2223 wire produced by American Superconductor (AMSC). This material is commercially available in lengths greater than 100 meters, and its specifications are as follows:

Min. I_c^*	115 A to 135 A
Average thickness	$t_T = 0.30 \text{ mm} \pm 0.02 \text{ mm}$
Stainless steel strip thickness	$t_{SS} = 37 \cdot 10^{-3} \text{ mm}$
Average width	$w_T = 4.16 \text{ mm} \pm 0.02 \text{ mm}$
Min. critical bend diameter	$D_{MIN} = 50 \text{ mm}$
Max. rated tensile strain **	$\epsilon_{MAX} = 0.35 \%$

* At 77 K, self-field, $1 \mu\text{V/cm}$

** With 95% I_c retention

Fig. 4 shows a cross section of an AMSC BSCCO-2223 Ag-sheathed High Strength tape.

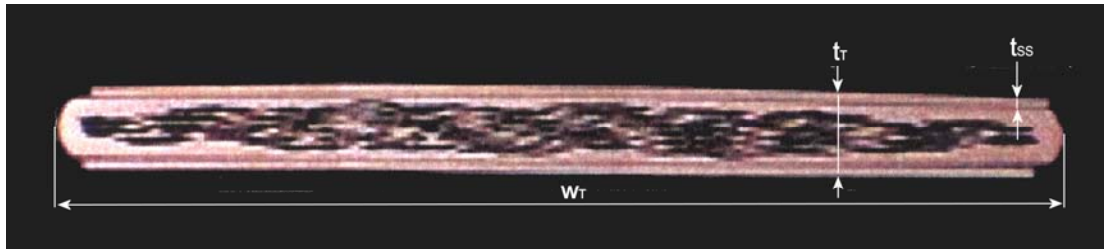


Fig. 4. Cross section photomicrograph of High Strength BSCCO2223 wire showing 37 μm thin strips of stainless steel on the top and bottom of the tape. The superconducting filaments are embedded in a Ag matrix.

The BSCCO-2223 tape was tested in both a hairpin and a spiral configuration. The last one was chosen to avoid the excessively sharp bends that caused some delamination of the tape in the hairpin configuration. The sample was soldered along all of its length on a G-10 cylindrical barrel wrapped with a brass sheet. The maximum bending strain on the sample was calculated to be 0.55% due to the bend diameter being 32 mm. The critical current measurement is performed as follows: a current is ramped up in the sample from zero. The sample is immersed in helium (liquid or vapor) in the cryostat Variable Temperature Insert, which is itself located in a solenoidal magnetic field. Voltages are measured at different points of the sample by means of voltage taps. As long as the sample is superconducting, the voltage measured between two taps is close to zero. It slowly begins to increase during transition to the normal state and finally shoots up at the critical current, I_c , as shown in Fig. 5, where the voltage-current curve was obtained at 14 K and 7 T. These measurements are carried out at different magnetic fields, up to 15 T, and at various temperatures. The magnetic field was in the long transverse direction parallel to the tape surface. Fig. 6 shows I_c results as a function of magnetic field for a BSCCO tape sample tested from 4.2 K up to 38 K. After comparison of these results with the company's data, it was found that strain affects I_c performance in the low field and low temperature range only. The I_c excess degradation due to strain was 17% at 22 K and 0 T, but only about 3% at larger fields. At 38 K no excess I_c degradation was observed due to strain. Fig. 7 shows the I_c as a function of temperature for the same sample tested from 0 T up to 15 T. As can be seen, the I_c data in Figure show a linear behavior with temperature, which is to be expected.

In order to make the best-informed decision on the superconductor to be used in this application, the performance of HTS and of Nb_3Sn can be compared in the form of engineering critical current density, J_E , in the field and temperature range of interest. Fig. 8 shows such a comparison at 4.2 K, and Fig. 9 at 14 K. The NbTi strand whose data are shown in Fig. 8 is a 0.8 mm strand developed for the SSC. The Nb_3Sn data are associated with 0.7 mm strands produced by Oxford Superconducting Technologies (OST) with the Modified Jelly Roll (MJR) and Restacked Rod Process (RRP). Their non-Cu critical current densities at 4.2 K and 12 T are $\sim 2000 \text{ A/mm}^2$ and $\sim 3000 \text{ A/mm}^2$ respectively. From these plots, the superiority of HTS materials is obvious at the higher temperatures, whereas at 4.2 K Nb_3Sn performs better at least up to magnetic fields of 17 T. The operation temperature eventually chosen for this project will therefore determine the superconductor of choice.

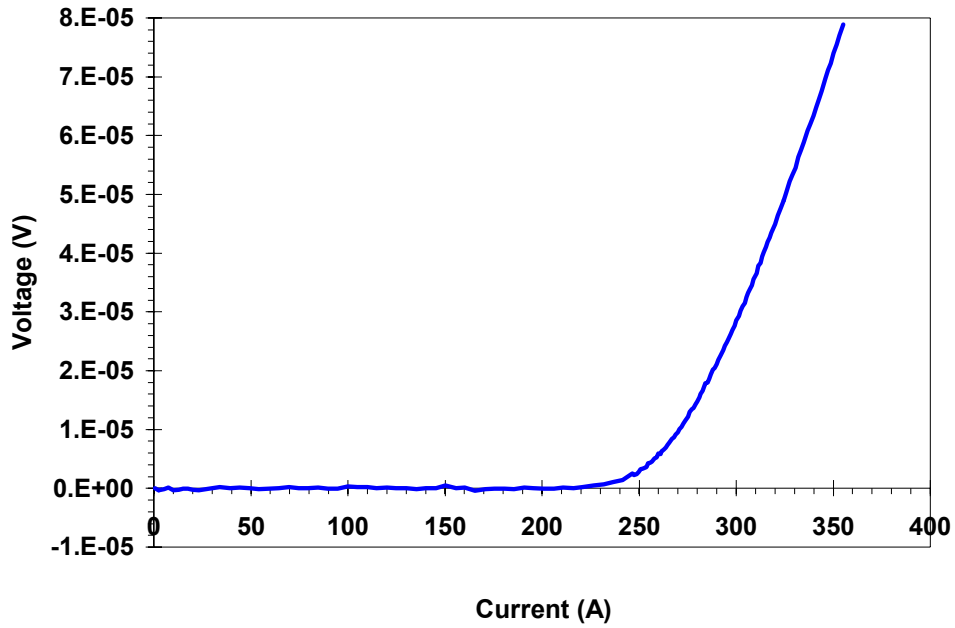


Fig. 5. Voltage-Current (VI) characteristics of High Strength BSCCO2223 wire tested at 14 K and 7 T.

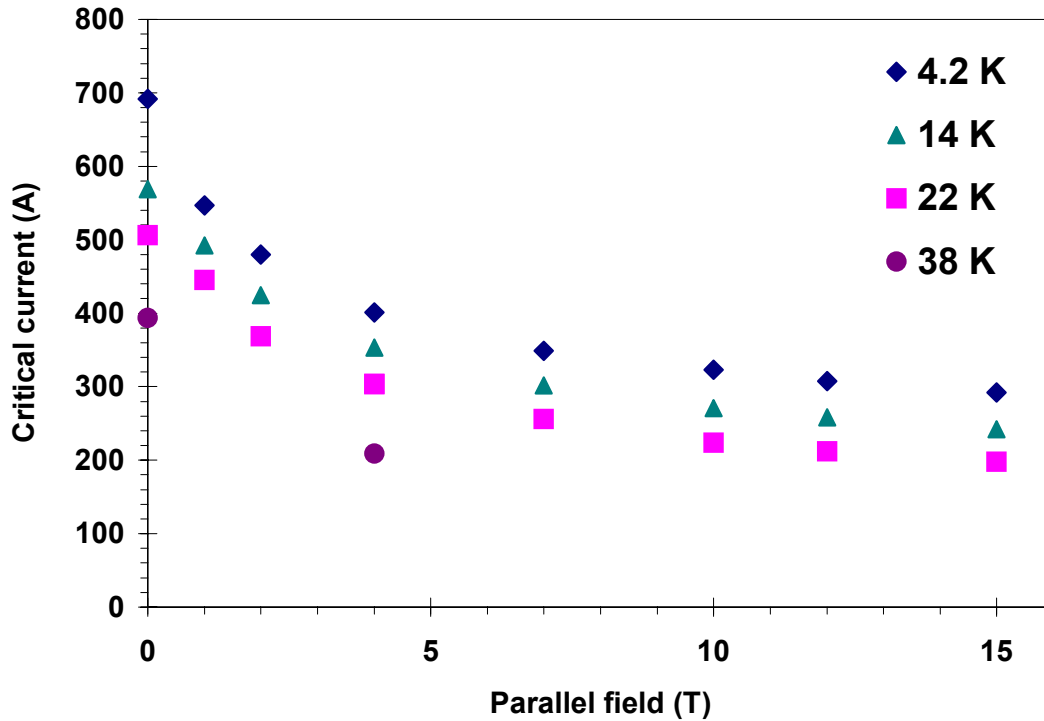


Fig. 6. Critical current as a function of magnetic field for a BSCCO tape sample tested in a parallel field configuration from 4.2 K up to 38 K.

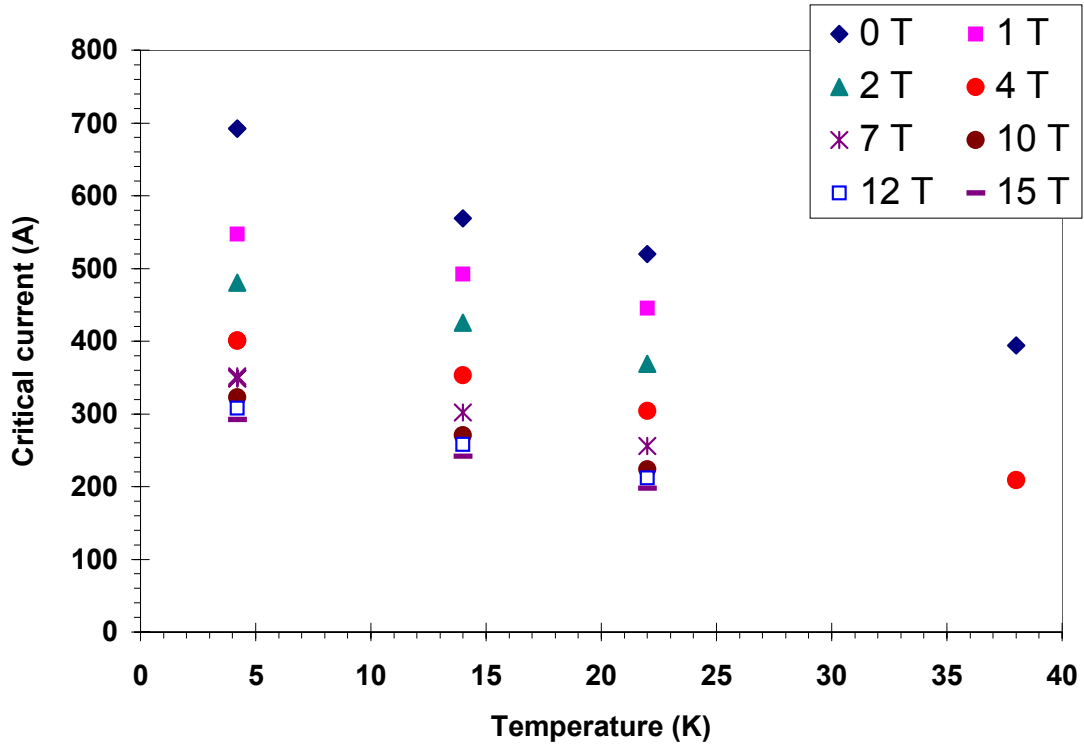


Fig. 7. Critical current as a function of temperature for a BSCCO tape sample tested in parallel field from 0 T up to 15 T.

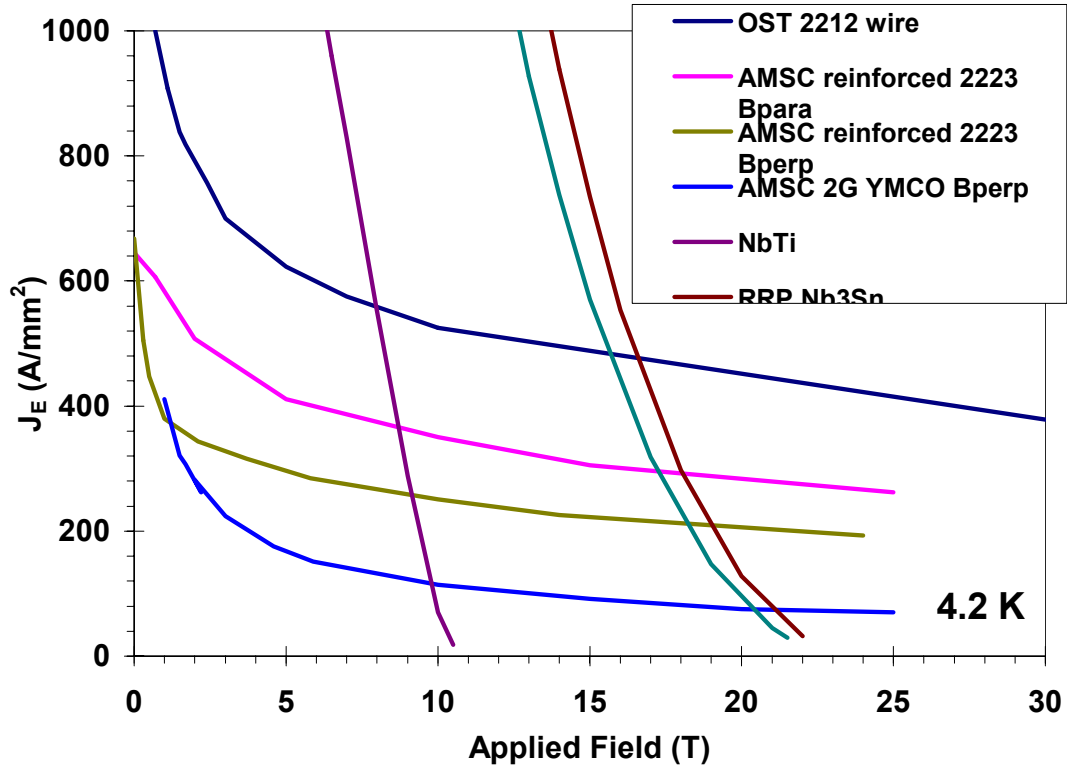


Fig. 8. Comparison of the engineering critical current density, J_E , at 4.2 K as a function of magnetic field between various HTS and Nb_3Sn materials.

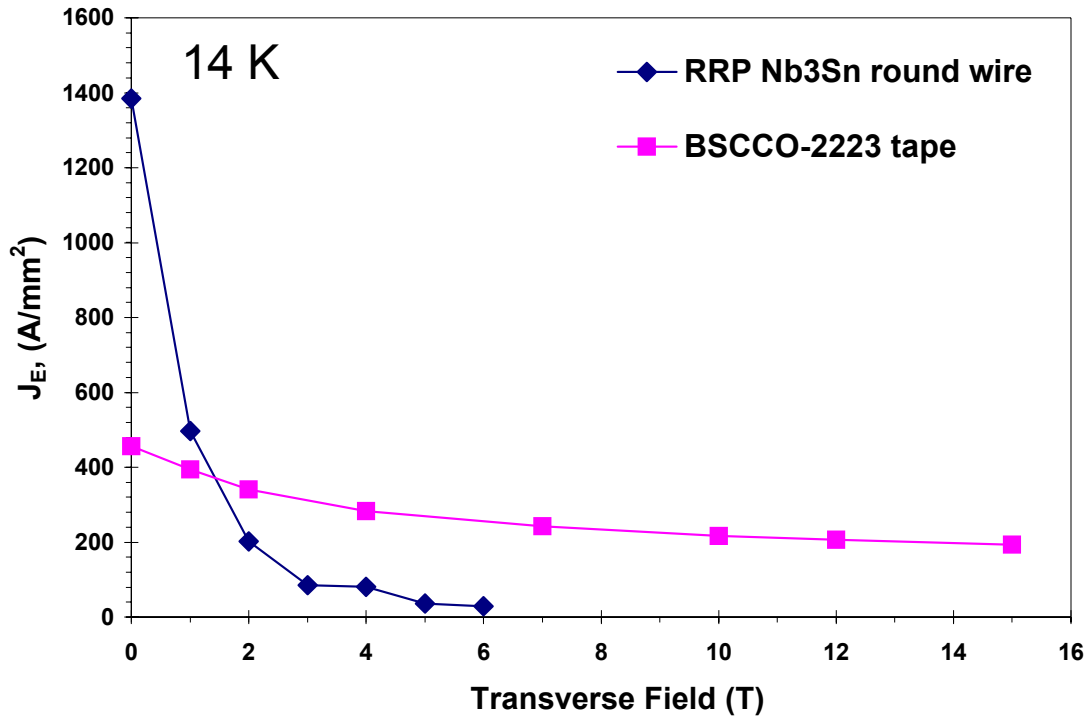


Fig. 9. Comparison of the engineering critical current density, J_E , at 14 K as a function of magnetic field between BSCCO-2223 tape and RRP Nb₃Sn round wire.

Work in progress and future plans

Whereas the first BSCCO tape measurements in parallel magnetic field were performed after modifying existing sample holders, new sample holders have been specifically designed and are being fabricated to test HTS tapes and wires in various field configurations, and with no strain on the sample. In addition to studying BSCCO-2223 tapes by AMSC, samples of the higher performance BSCCO-2212 round wire by OST are being heat treated by the company and will also be tested soon. Studies of strain effects on the superconducting properties will also be performed to confirm the finding that strain affects I_c performance in the low field and low temperature range only. This will help determine whether a React&Wind or Wind&React technology should be used for the superconducting magnets. Once the operation temperature and magnetic field operation range of the application in this proposal will have been specified, magnetization measurements might be of interest too. If HTS materials will be chosen for the magnets of a HCC, resources will have to be spent in setting up an appropriate heat treatment site for reaction in oxygen atmosphere, and R&D will have to be performed on thermal cycle optimization of these materials.

Appendix X – Tabletop RF Breakdown Apparatus

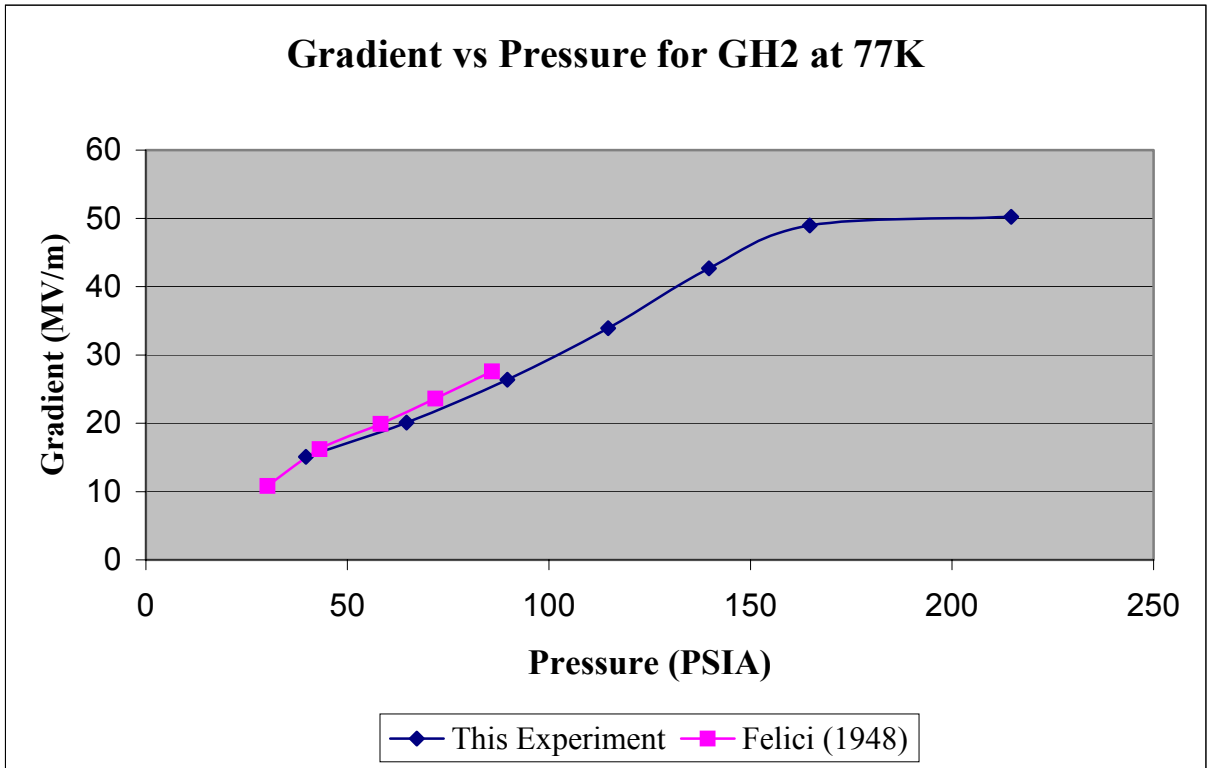


Figure X.1. First copper breakdown measurements in hydrogen gas at Lab G at 800 MHz compared to DC measurements taken in 1948 normalized to the same gas density. The similarity of the results has inspired the idea that the table-top device described below to study DC breakdown in gases and metals could be an advantage.

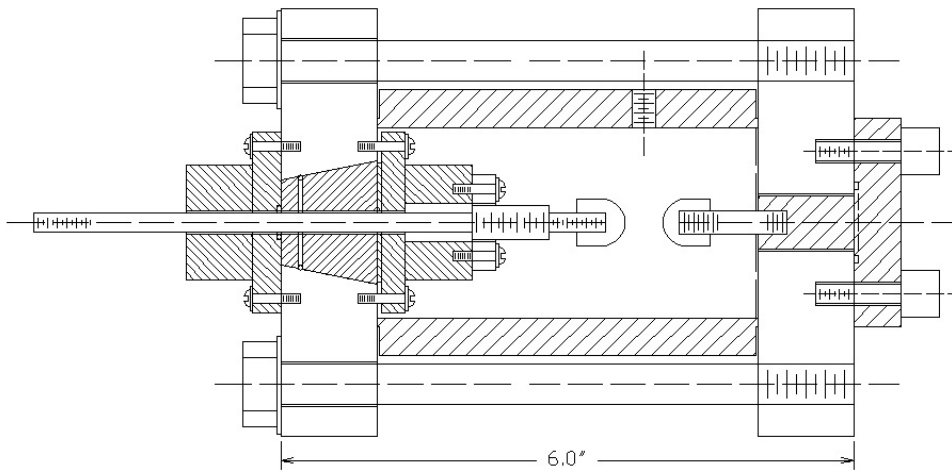


Figure X.2. High-pressure test cell to study the breakdown of gases and metals. Metallic hemispherical electrodes are caused to breakdown using an automobile ignition coil.

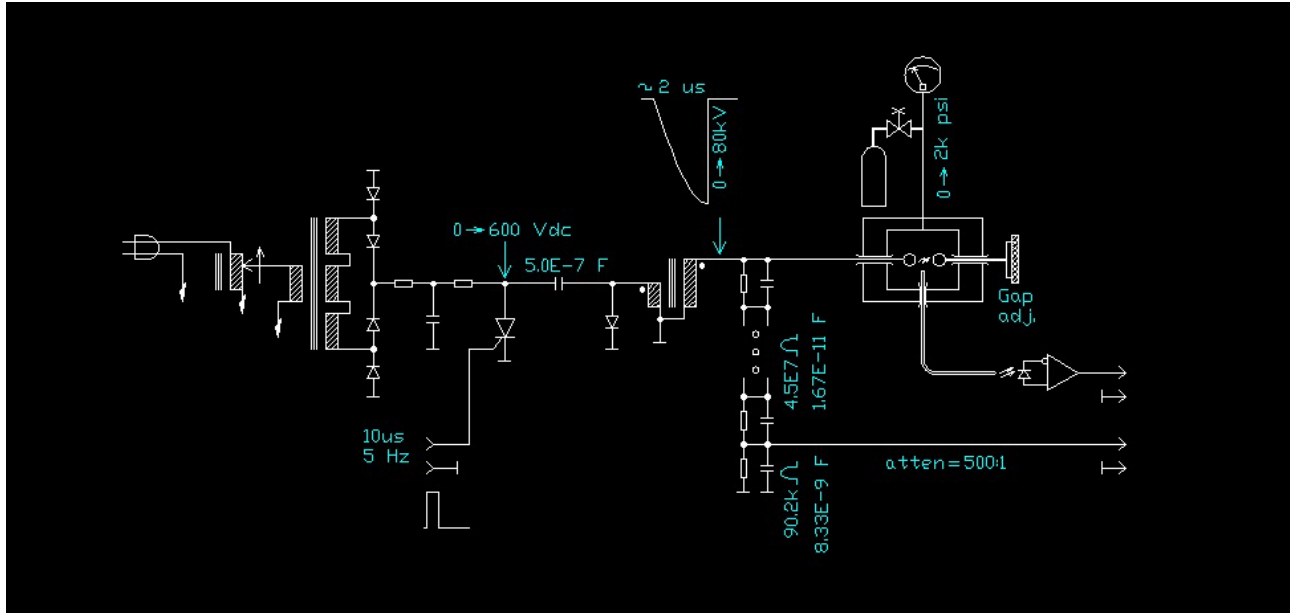
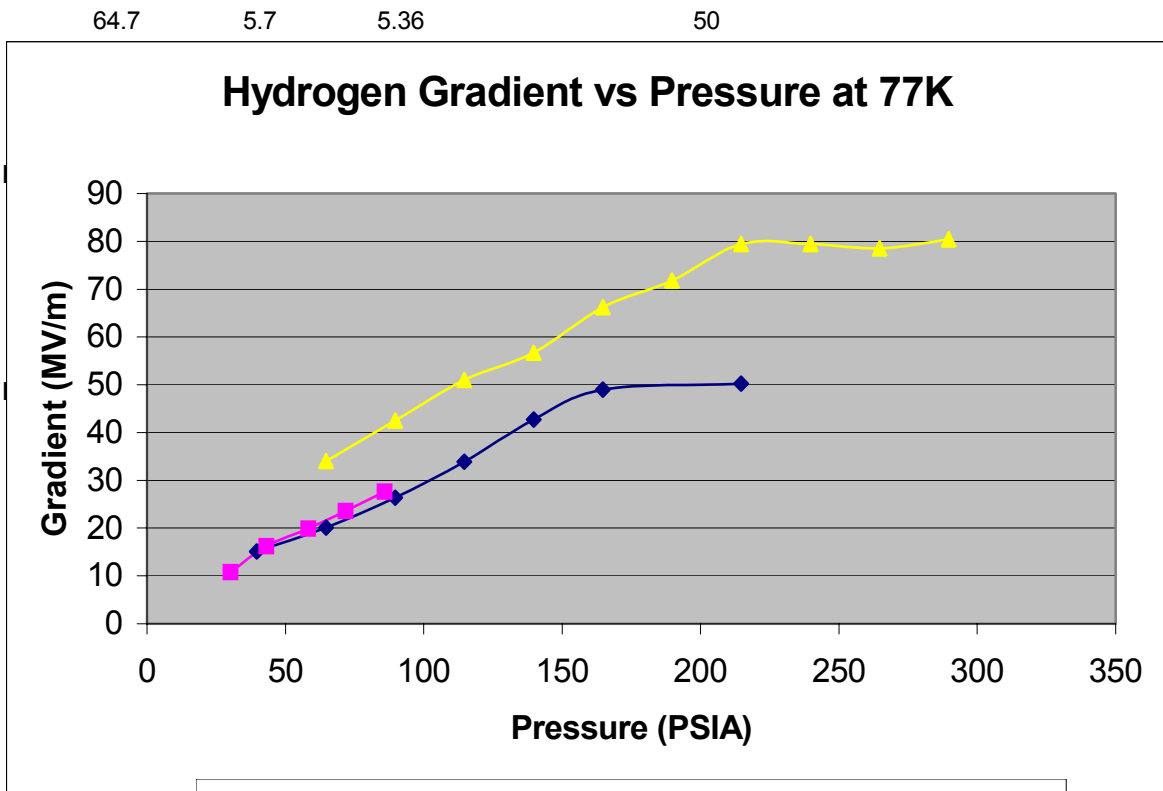


Figure X.3. Ignition coil circuit for the breakdown apparatus shown in figure X.2.





First measurements from the desk-top experiment are shown in yellow and scaled by temperature to compare with the density of the Lab G measurements.

Appendix XI- Cryostat Schematics

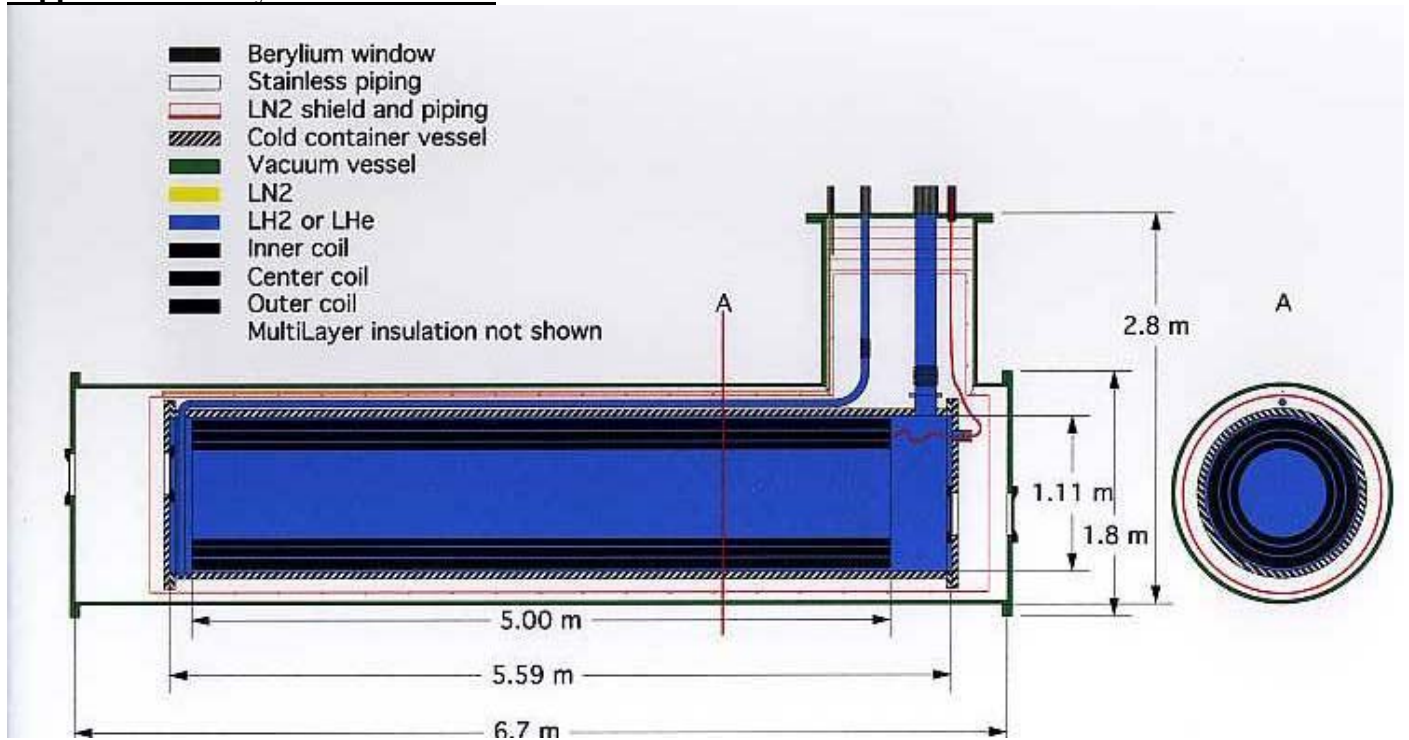


Figure XI.1. First schematic of a cryostat for the MANX experiment.

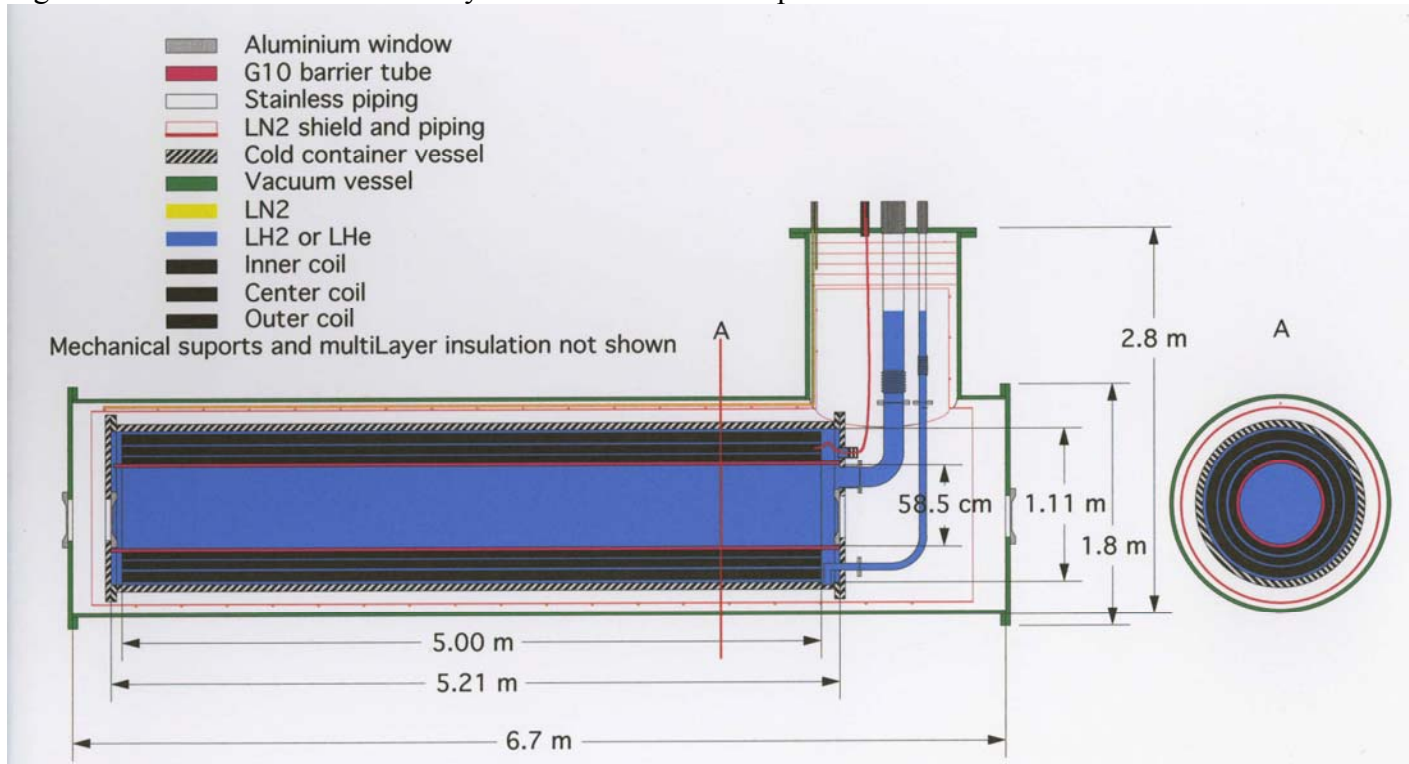


Figure XI.2. Second iteration of MANX cryostat schematic showing improvements and simplifications. Here, cold liquid H_2 or He is forced through the HTS (16 K) or Nb_3Sn (2 K) coils before entering the region where the beam can heat the liquid. The insulated G10 barrier keeps the coils at constant temperature, independent of the beam heating in the central volume.